A Study of the Products of the Gas-Phase Reactions $M + N_2O$ and $M + O_3$, where M = Na or K, with Ultraviolet Photoelectron Spectroscopy

1992

by

Timothy G. Wright, Andrew M. Ellis and John M. Dyke*

Department of Chemistry
The University
Southampton
SO9 5NH
U.K.

* to whom correspondence should be addressed

-AQ # M97-03-1723

PLEASE CHECK THE APPROPRIATE BLOCK BELOW:

☐ ________ copies are being forwarded. Indicate whether Statement A, B, C, D, E, F, or X applies.

☑ DISTRIBUTION STATEMENT A:
APPROVED FOR PUBLIC RELEASE: DISTRIBUTION IS UNLIMITED

☐ DISTRIBUTION STATEMENT B:
DISTRIBUTION AUTHORIZED TO U.S. GOVERNMENT AGENCIES ONLY; (Indicate Reason and Date). OTHER REQUESTS FOR THIS DOCUMENT SHALL BE REFERRED TO (Indicate Controlling DoD Office).

☐ DISTRIBUTION STATEMENT C:
DISTRIBUTION AUTHORIZED TO U.S. GOVERNMENT AGENCIES AND THEIR CONTRACTORS; (Indicate Reason and Date). OTHER REQUESTS FOR THIS DOCUMENT SHALL BE REFERRED TO (Indicate Controlling DoD Office).

☐ DISTRIBUTION STATEMENT D:
DISTRIBUTION AUTHORIZED TO DoD AND U.S. DoD CONTRACTORS ONLY; (Indicate Reason and Date). OTHER REQUESTS SHALL BE REFERRED TO (Indicate Controlling DoD Office).

☐ DISTRIBUTION STATEMENT E:
DISTRIBUTION AUTHORIZED TO DoD COMPONENTS ONLY; (Indicate Reason and Date). OTHER REQUESTS SHALL BE REFERRED TO (Indicate Controlling DoD Office).

☐ DISTRIBUTION STATEMENT F:
FURTHER DISSEMINATION ONLY AS DIRECTED BY (Indicate Controlling DoD Office and Date) or HIGHER DoD AUTHORITY.

☐ DISTRIBUTION STATEMENT X:
DISTRIBUTION AUTHORIZED TO U.S. GOVERNMENT AGENCIES AND PRIVATE INDIVIDUALS OR ENTERPRISES ELIGIBLE TO OBTAIN EXPORT-CONTROLLED TECHNICAL DATA IN ACCORDANCE WITH DoD DIRECTIVE 5230.25, WITHHOLDING OF UNCLASSIFIED TECHNICAL DATA FROM PUBLIC DISCLOSURE, 6 Nov 1984 (Indicate date of determination). CONTROLLING DoD OFFICE IS (Indicate Controlling DoD Office).

☐ This document was previously forwarded to DTIC on ________ (date) and the AD number is ____________.

☐ In accordance with provisions of DoD instructions, the document requested is not supplied because:

☐ It will be published at a later date. (Enter approximate date, if known).

☐ Other. (Give Reason)

DoD Directive 5230.24, "Distribution Statements on Technical Documents," 18 Mar 87, contains seven distribution statements, as described briefly above. Technical Documents must be assigned distribution statements.

DAVE ROMINE
Print or Type Name

Joyce Chiras
Authorized Signature/Date

99-011-44-171-514-4950
Telephone Number

Abstract

Products of the gas-phase reactions M + N_2O and M + O_3, where M = Na or K, have been investigated with u.v photoelectron spectroscopy and bands have been assigned with the assistance of results from *ab initio* molecular orbital calculations.

For the M + N_2O reactions, the observed products were MO + N_2. Measurement of the photoelectron bands associated with the metal monoxide, MO, allowed determination of the first adiabatic ionization energies of NaO and KO. The values obtained were AIE[NaO($X^2\Pi$)] = (7.1 ± 0.1) eV and AIE[KO($X^2\Pi$)] = (6.9 ± 0.1) eV. A similar study of the Li + N_2O reaction gave AIE[LiO($X^2\Pi$)] = (7.6 ± 0.2) eV.

The reactions M + O_3, with M = Na or K, were observed to give MO + O_2 as the major reaction products. However, for each reaction a band was observed which was assigned to the first ionization energy of the secondary reaction product, MO_2. From the spectra obtained, the first adiabatic ionization energies of NaO_2 and KO_2 were measured as AIE[$NaO_2(\tilde{X}^2A_2)$] = (6.2 ± 0.2) eV and AIE[$KO_2(\tilde{X}^2A_2)$] = (5.7 ± 0.1) eV.

For both the M + N_2O and M + O_3 reactions, production of MO $A^2\Sigma^+$ was found to be favoured relative to production of the MO $X^2\Pi$ state, a result which has important implications in understanding the sodium night-glow in the mesosphere.

Introduction

The alkali metal oxides and their singly-charged cations are of importance in atmospheric chemistry (1-8) as well as in energy technology (9) and flame chemistry (10-13). NaO is also involved in reactions that form the basis of the $Na/N_2O/CO_2$ chemical laser (14).

The mesospheric sodium night-glow is believed to be produced from the chemiluminescent reaction of sodium monoxide with atomic oxygen, sodium monoxide being formed by the reaction of atomic sodium with ozone (1-8). Chapman proposed a simple mechanism to explain this chemiluminescent phenomenon by postulating a scheme whereby atomic sodium catalyzes the reaction of atomic oxygen with ozone to form two diatomic oxygen molecules (3). As the ability to accurately model Chapman's mechanism depends on the availability of reliable rate constants for the reactions involved, the kinetics of atmospherically important reactions involving sodium have been studied in some detail in the last fifteen years (15-17).

Despite the importance of the alkali metal oxides, relatively few spectroscopic studies have been made on these species in the gas-phase. Mass-spectrometric experiments, using electron impact ionization, have shown that the vapour above heated $Na_2O(s)$ consists mainly of Na(g) and $O_2(g)$ with NaO(g) and $Na_2O(g)$ being minor constituents (18,19). However, these results have recently been disputed (20). It was argued in reference (20) that the dissociative nature of NaO_2^+ led to an incorrect analysis of the electron impact mass spectrometric data in references (18) and (19), and that $NaO_2(g)$ is a major constituent of the vapour above heated $Na_2O(s)$.

The first ionization energy of NaO has been measured in electron impact mass spectrometric studies as (6.5 ± 0.7) eV (19) and 7.41 eV (21). As well as mass spectrometric studies, NaO^+ has been detected in merging beam reactions of sodium with some selected atmospheric molecular ions (22-24).

Also, highly excited NaO has been deduced to be formed in crossed-beam studies of electronically excited sodium with O_2 (25).

Very little thermodynamic data exists for potassium oxides in the gas-phase (26,27). There have been some electron impact mass spectrometric studies which yielded values of 7.1 ± 0.2 eV (26), and 7.5 eV (21) for the first ionization energy of KO. An electron impact mass spectrometric study by Ehlert (26) obtained a value for the first ionization energy of K_2O as 7.5 ± 0.2 eV, whereas the work of reference (21) gave 4.96 eV. As these values are clearly very different from each other, one of them must be in error. If the first ionization energy of Na_2O is considered, then three separate determinations have yielded 5.5 ± 0.5 eV (19), 5.35 eV (22), and 5.06 ± 0.10 eV (28). Since the first ionization energies of atomic sodium and potassium are 5.14 and 4.34 eV respectively (29), it seems that 4.96 eV is the more reliable value for the first ionization energy of K_2O, as the first ionization energies of Na and Na_2O are very close to each other.

Studies have also been performed on the chemiluminescence emitted in the gas-phase reaction of an alkali metal with N_2O or O_3 (30,31). In these experiments, the observed chemiluminescence was assigned to a weakly-bound excited metal monoxide Π-state emitting to the lowest Π-state. A mechanism for the formation of this excited state has recently been suggested (32) since it has been noted (33) that the excited Π-state is thermodynamically inaccessible from ground state reactants for the reactions involving sodium. As well as gas-phase studies, matrix isolation studies have been performed on the alkali metal oxides (34-39).

One of the most interesting features of the alkali monoxides is that they undergo a change in electronic ground state as the group is descended. For LiO and NaO, the ground state has been conclusively shown to be $^2\Pi$ by both experimental (40-42) and theoretical methods (43-50). In contrast, RbO and

CsO have been shown to have $^2\Sigma^+$ ground states (40,47-49,51,52). The ground state of KO was uncertain until gas-phase microwave studies showed it to be a $^2\Pi$ state with a $^2\Sigma^+$ state lying 202 cm^{-1} higher in energy (53). Similar microwave spectroscopic measurements have shown that the ground state is $^2\Pi$ for LiO (54) and NaO (55), in agreement with the results of previous work. The energy difference between the $X^2\Pi$ and $A^2\Sigma^+$ states was derived from these microwave measurements as 2565 and 2050 cm^{-1} for LiO and NaO respectively.

The amount of work performed on the alkali metal monoxide cations is much less than that on the neutral species. The first observation of NaO^+ and KO^+ was by Rol and Entemann (22) in merging beam studies of sodium and potassium in collision with atmospheric ions. Subsequently, from the energy dependence of the cross-sections of the reactions of Na and K with CO^+, the dissociation energies of NaO^+ and KO^+ were derived as (0.8 ± 0.3) eV and (0.3 ± 0.3) eV respectively (24). No other experimental studies on the alkali metal monoxide cations appear to have been reported.

A substantial amount of experimental work has been performed on lithium oxides. The vapour above heated $Li_2O(s)$ has been studied by White *et al.* (56) by electron impact mass spectrometry and values for the first ionization energies of LiO and Li_2O have been reported as (8.6 ± 0.3) eV and (6.9 ± 0.3) eV. A number of other studies of this type have also been performed . These gave the first ionization energy of LiO as (9.0 ± 0.2) eV (57), (8.45 ± 0.20) eV (58) and (8.96 ± 0.20) eV (59) and the first ionization energy of Li_2O as (6.8 ± 0.2) eV (57), (6.19 ± 0.20) eV (58) and (6.41 ± 0.20) eV (59). It is interesting to note that, as appears to be the case for Na_2O, the first ionization energy of Li_2O is higher than that of the atomic metal, (5.390 eV (29)) . A number of matrix isolation studies on lithium oxides have also been carried out (56,60-65). These have allowed measurement of the vibrational frequencies and estimation of the equilibrium geometries of the metal oxides studied.

Only a small number of calculations have been performed on the alkali metal oxides to derive ionization energies. SCF *ab initio* calculations on $NaO(X^2\Pi)$ and $NaO^+(X^3\Sigma^-)$, using a double-zeta plus polarization STO basis set, gave the first adiabatic and vertical ionization energies of NaO as 7.4 and 7.7 eV respectively (43). Calculations on the ionization energies of some lithium oxides have also been reported (44).

In the present work, it was proposed to record the HeI photoelectron spectra of NaO and KO prepared by the gas phase reactions

$$M + O_3 \rightarrow MO + O_2 \quad \ldots\ldots\ldots\ldots \quad (1)$$

$$M + N_2O \rightarrow MO + N_2 \quad \ldots\ldots\ldots\ldots \quad (2)$$

where M = Na or K.

The preparation of the metal monoxides for p.e.s. study via a gas-phase reaction was necessary since, as noted above, mass spectrometric studies have shown that alkali metal monoxides are minor species in the vapour above heated solid alkali metal oxides. The room temperature rate constant for the Na + O_3 reaction is known to be high (33,66-68). Unfortunately, the rate constant for reaction (1) with M=K has not yet been measured although it is exothermic and is expected to be fast by analogy with the known rate constant of the sodium reaction. Reaction (2) is known to be rapid at room temperature for both sodium (67-70) and potassium (71). Photoelectron spectra recorded for both reactions (1) and (2), with M=Na or K, should provide confirmation that the spectra obtained can be associated with the metal monoxides. Some preliminary p.e.s. were also performed on the Li + N_2O reaction.

Experimental

The spectra obtained in this work were recorded on a high temperature, single detector photoelectron spectrometer which has been described previously (72,73). The metals were vaporized using radiofrequency induction heating from stainless steel furnaces, which contained a molybdenum capillary to collimate the metal beam.

Ozone was prepared prior to each experiment from a silent electric discharge through very slowly flowing molecular oxygen. It was separated from oxygen by trapping it on non-indicating silica gel in a U-tube placed in a dry ice/acetone slush bath at 196K (74,75). The presence of ozone could easily be monitored, as the gel turned a deep mauve colour as the ozone was trapped. A dry ice/acetone slush bath maintained a constant temperature for 4-5 hours before refilling was necessary and typically it took about six hours to obtain sufficient trapped ozone for a single photoelectron experiment.

In order to improve the mixing of the metal vapour with ozone, a reaction cell was used in front of the entrance slits of the spectrometer. This reaction cell also allowed higher local pressures of ozone to be used in the region of the photon beam than would otherwise have been possible. A diagram of this reaction cell is shown in Figure 1.

Figure 1

As may be seen, the metal enters the reaction cell from the top and the ozone enters from the side opposite the HeI_{α} (21.22 eV) photon source. In order to obtain a metal vapour beam with sufficiently high partial pressure in the reaction cell to allow metal oxide spectra to be recorded, the radiofrequency inductively heated furnace had to be positioned within $\approx$ 1 cm of the top of the reaction cell.

Computational Details : Alkali Monoxides

In this work, *ab initio* RHF and CISD calculations were performed on the low-lying neutral and ionic states of the alkali monoxides NaO and KO using basis sets of approximately triple zeta plus polarization quality.

For sodium, a [8s7p] contraction of the (12s9p) basis set of McLean and Chandler (76) was used, supplemented with one set of d functions (77). The potassium basis set was a [12s9p] contraction of the (14s11p) basis set of Wachters (78), supplemented with one set of d functions, derived from reference (77). The oxygen basis set was a [5s3p] contraction of the (7s3p) basis of Roos and Siegbahn (79), supplemented with a set of diffuse p functions (80) and a set of d functions (77).

In the CISD scheme, all electrons and orbitals were included, and the effects of quadruple excitations were allowed for using the Davidson correction (81). All calculations on the alkali metal monoxides were performed using the GAMESS package of programs (82).

The energy of each neutral or ionic state was calculated at a series of bond lengths close to the minimum and then spectroscopic constants were derived by fitting a potential curve to these values. Details of the fitting procedure used are given in reference (83). Once the equilibrium bond length had been derived from this fit, a further calculation was carried out at this bond length in order to obtain the energy of that state at the computed minimum; this allowed the calculation of adiabatic ionization energies (AIEs). In order to calculate vertical ionization energies (VIEs), calculations on the ions were performed at the computed equilibrium bond lengths of the neutral molecules. In a related study, an investigation of the effects of basis set superposition error on computed equilibrium bond lengths and vibrational frequencies for the $X^2\Pi$ and $A^2\Sigma^+$ states of NaO and KO has been recently performed (50).

The outermost electronic configurations of the two lowest electronic states of the alkali metal monoxides are:-

$\pi^3\sigma^2$ .... $^2\Pi$

$\pi^4\sigma^1$ .... $^2\Sigma^+$,

where the σ and π orbitals are essentially oxygen 2p orbitals. These two states simply arise from positioning the unpaired electron along the internuclear axis ($^2\Sigma^+$ state) or perpendicular to this axis ($^2\Pi$ state).

One-electron ionization from the outermost σ and π orbitals of the $^2\Pi$ state give rise to five ionic states; $^3\Sigma^-$, $^1\Delta$ and $^1\Sigma^+$ states resulting from the π^{-1} ionization, and $^3\Pi$ and $^1\Pi$ ionic states resulting from the σ^{-1} ionization. One electron ionization from the $^2\Sigma^+$ state gives rise to the same $^3\Pi$ and $^1\Pi$ states via the π^{-1} ionization and another $^1\Sigma^+$ state is obtained from the σ^{-1} ionization.

In this work, the calculations described above were performed for all six ionic states. Vertical and adiabatic ionization energies to these ionic states from both the $X^2\Pi$ and $A^2\Sigma^+$ neutral states were calculated, provided each ionization is allowed on the basis of the one-electron ionization selection rule.

Calculated Equilibrium Bond Lengths (r_e) and Vibrational Frequencies ($\bar{\omega}_e$) for MO($X^2\Pi$) and MO($A^2\Sigma^+$) (M = Na or K).

The calculated values for r_e and $\bar{\omega}_e$ obtained for NaO($X^2\Pi$) and NaO($A^2\Sigma^+$) are shown in Tables 1 and 2 respectively. The corresponding values calculated for KO($X^2\Pi$) and KO($A^2\Sigma^+$) are listed in Tables 3 and 4. Also shown are the results of previous calculations and the available experimental values.

Tables 1 to 4

In general, the agreement with experimental values is reasonably good, particularly (probably fortuitously so) at the SCF level. Good agreement with the results of some previous calculations (48) is also obtained. This agreement is satisfying because the previous calculations (48) used very large STO basis sets, whereas the present calculations employ basis sets of approximately TZ + P quality. The results presented in Tables 1 to 4 have been discussed in detail elsewhere (50). They are presented here for comparison with the corresponding ionic state values.

Photoelectron Spectra recorded for the Na + N_2O and Na + O_3 reactions

The HeI photoelectron spectrum recorded for the Na + N_2O reaction in the ionization energy region 5.0-9.5 eV is shown in Figure 2. This figure shows three resolved bands (labelled A, B and C) which are associated with reaction products. One notable feature of the spectrum is the sharp cut-off to high ionization energy at approximately 8.35 eV.

The photoelectron spectrum recorded for the Na + O_3 reaction in the same ionization energy region is shown in Figure 3. In this case four bands (labelled A, B, C and D) were observed associated with reaction products. A summary of the measured vertical ionization energies (VIEs) of the bands, observed from the two preparative routes is shown in Table 5. Calibration of these spectra was achieved using the position of the $(3s)^{-1}$ ionization of sodium (29) and the position of the first band of methyl iodide (84), which was added as a calibrant. As N_2 and O_2, products of the Na + N_2O and Na + O_3 reactions respectively, have photoelectron bands at higher ionization energy than the region shown in Figures 2 and 3, it is clear that Bands A to D must be associated with NaO or possibly some other oxide of sodium which arises from a secondary reaction involving NaO.

The results of the *ab initio* calculations of the NaO vertical and adiabatic ionization energies (VIEs and AIEs) are shown in Tables 6 and 7. Ionic equilibrium bond lengths (r_e) and vibrational frequencies ($\bar{\omega}_e$) as calculated using the fitting procedure described earlier (83) are also presented in these tables.

Figure 2

Tables 5, 6 and 7

Although reaction (2) with M=Na is known to be rapid, the secondary reaction

$$NaO + N_2O \rightarrow NaO_2 + N_2 \quad \ldots\ldots\ldots\ldots\ldots\ldots \quad (3)$$

is much slower (67). Hence, the reaction product bands A, B and C, shown in Figure 2, were associated solely with ionization of NaO. Assignment of these bands was, however, not straightforward. Although it is established that the electronic ground state of NaO is a $^2\Pi$ state, a $^2\Sigma^+$ lies only $\approx$ 2000 cm^{-1} (0.25 eV) higher (55) and is accessible in the exothermic reaction, reaction (2), used to prepare NaO. In fact, the exothermicity of reaction (2) with ground state reactants and products (i.e. yielding NaO($X^2\Pi$)), can be calculated using available heats of formation (85) as -1.09 eV and the reaction, like that leading to formation of NaO($A^2\Sigma^+$), is 'allowed' on the basis of Wigner-Witmer correlation rules (86). Hence, there is the possibility of both $X^2\Pi$ and $A^2\Sigma^+$ states of NaO contributing to the photoelectron spectrum. If ionization from the $^2\Pi$ state is considered, then it may be seen from Table 6 that the two lowest ionizations are to the $X^3\Sigma^-$ and $A^3\Pi$ ionic states. Ionization energies to other accessible states are expected to be greater than 1 eV above the ionization energies to these states. Thus the fact that there are three bands within 0.5 eV in the experimental spectrum suggests that one of the bands originates from the $A^2\Sigma^+$ state of NaO. In fact, inspection of Table 7 shows that the $NaO^+(A^3\Pi) \leftarrow NaO(A^2\Sigma^+)$ ionization occurs in the same ionization energy region as the $NaO^+(A^3\Sigma^-) \leftarrow NaO(X^2\Pi)$ and $NaO^+(A^3\Pi) \leftarrow NaO(X^2\Pi)$ ionizations. Thus the three photoelectron bands, A, B and C, are assigned to these processes. The photoelectron bands arising from ionization to the higher ionic states shown in Tables 6 and 7 will be weaker than bands A to C, since they arise from ionization to singlet states.

No higher NaO bands were observed because the experimental photoelectron spectra became complex above 9.5 eV ionization energy because of intense HeIβ

bands from N_2O, O_2 and O_3.

Since no vibrational structure was resolved in bands A, B and C, the assignment of the observed bands in the Na + N_2O reaction was made purely on the basis of computed vertical ionization energies. The assignment can be summarised as follows:-

Band A : $NaO^+(X^3\Sigma^-) \leftarrow NaO(X^2\Pi)$
Band B : $NaO^+(A^3\Pi) \leftarrow NaO(A^2\Sigma^+)$
Band C : $NaO^+(A^3\Pi) \leftarrow NaO(X^2\Pi)$

The band intensity ratio A:C in all the Na + N_2O experimental spectra was approximately 1:2, which is consistent with this assignment.

Since all the above ionizations essentially involve removal of an O 2p electron from an ionic neutral molecule, Na^+O^-, the photoionization cross-sections for each ionization will be approximately the same. The relative intensities of bands A, B and C will, therefore, be controlled by the degeneracy of the neutral and ionic states involved and the population of the $X^2\Pi$ and $A^2\Sigma^+$ states on ionization. Experimentally, the intensities of bands B and C were approximately equal in most spectra. As the final ionic state is the same in each case, this implies that the population of the $A^2\Sigma^+$ state is approximately twice that of the $X^2\Pi$ state on photoionization, as the degeneracy of the $^2\Pi$ state is twice that of the $^2\Sigma^+$ state. In fact, in some Na + N_2O spectra band B was more intense than band C with the maximum measured ratio being approximately 2:1. This implies that a maximum $A^2\Sigma^+$:$X^2\Pi$ population ratio of 4:1 was observed in this work, although most spectra were consistent with a population ratio of 2:1. This result of a preferential population of the $A^2\Sigma^+$ NaO state relative to the $X^2\Pi$ state from the Na + N_2O reaction is consistent with the work of Kolb, Herschbach and co-workers (7,8) who have shown, by molecular beam magnetic deflection experiments, that NaO is produced from the Na + O_3 reaction, almost exclusively in the $NaO(A^2\Sigma^+)$

state. A similar result is expected for the Na + N_2O reaction on the basis of the results of the present study. If in this present work, the $A^2\Sigma^+$ state of NaO is formed almost exclusively in the Na + N_2O reaction, then the $X^2\Pi$ state will be produced by collisional deactivation. This would then explain the observation that some spectra showed different B:C relative band intensities, although the ratio A:C was approximately constant.

Assuming that no vibrational excitation of NaO is present on ionization, the onset of band A corresponds to the first adiabatic ionization energy of NaO. The measured value, (7.1 ± 0.1) eV, is consistent with the calculated CISD + Q value obtained in this work of 6.78 eV and is in reasonable agreement with values obtained by electron impact mass spectrometry of (6.5 ± 0.7) eV (19) and 7.41 eV (21). The maximum of band A, (7.70 ± 0.06) eV, is also in reasonable agreement with the CISD + Q computed vertical ionization energy for the process $NaO^+(X^3\Sigma^-) \leftarrow NaO(X^2\Pi)$ of 7.10 eV.

The three NaO bands observed in the Na + N_2O spectra were also seen in spectra recorded for the Na + O_3 reaction (see Figure 3). These bands had the same vertical ionization energies as bands A, B and C in Figure 2 (see Table 5) and their relative intensities showed the same characteristics as the three bands observed from the Na + N_2O reaction. These bands were therefore attributed to the same NaO bands seen from the Na + N_2O reaction and, as in the Na + N_2O case, the spectra were consistent with production of the $A^2\Sigma^+$ state in preference to the $X^2\Pi$ state.

As well as the three bands seen from the Na + N_2O route, one other band was observed in the Na + O_3 spectra. This band (band D in Figure 3) is to lower ionization energy of the other bands, and cannot therefore be due to another ionization of the X or A states of NaO (see Table 5). However, the exothermicity of the Na + O_3 reaction (1.72 eV) is greater than that of the Na + N_2O reaction (1.09 eV) and the possibility that a higher state of NaO is contributing to the photoelectron spectrum must therefore be considered. However, recent calculations of Langhoff *et. al* (87) exclude this, as the next highest states of NaO are greater than 2 eV above the $X^2\Pi$ state. The assignment that is favoured here is that band D arises from ionization of NaO_2, produced from the secondary reaction

$$NaO + O_3 \rightarrow NaO_2 + O_2 \qquad \ldots\ldots\ldots\ldots \qquad (4)$$

Figure 3

The rate constant of this reaction has been measured as 2×10^{-10} cm^3 $molecule^{-1}$ sec^{-1} at 500K (66,69) and reaction 4 is much faster than the corresponding reaction of NaO with N_2O to give NaO_2 and N_2 (67).

To investigate the possibility of assigning band D to NaO_2, *ab initio* calculations were performed on NaO_2 and its low-lying ionic states. Analogous calculations were also performed for KO_2 as it is expected that in the $K + O_3$ reaction sequence, KO_2 would be produced via the secondary reaction $KO + O_3$ under the experimental conditions used.

Computational Details : Alkali Metal Superoxides

Calculations were performed on NaO_2 and KO_2 using the same basis sets as used in the calculations on NaO and KO. Since the effects of electron correlation are known to be important in the alkali metal monoxides (this work and refs. 46-50), and since the equilibrium geometries of the neutral alkali metal superoxides are not well established, it was decided to perform geometry optimization calculations at the RHF, UHF and (U)MP2 levels of theory. A C_{2v} geometry was assumed in most of these calculations as matrix-isolation infrared (34), Raman (36) and e.s.r. (51,88,98) spectroscopic studies have established that NaO_2 has an ionic $Na^+O_2^-$ structure of C_{2v} symmetry in its ground electronic state. Analytic gradient methods, as implemented in the CADPAC suite of programs (89), were used. At the RHF and MP2 levels of theory, use of analytic second derivatives allowed the calculation of harmonic frequencies. For UHF and UMP2 calculations, numerical force constant calculations were performed in order to obtain harmonic vibrational frequencies. Once the optimized geometries of the ground state neutral species had been determined, CISD calculations were performed at the UMP2 geometries of the neutral states for both the ground neutral and the low-lying ionic states. This allowed vertical ionization energies to be calculated, which could then be compared with the experimental values and the computed alkali monoxide values. Again, as in the alkali monoxide computations, all electrons were included in the CISD calculations, which were performed using the GAMESS suite of programs (82).

Calculated Equilibrium Geometries and Vibrational Frequencies for $NaO_2(\tilde{X}^2A_2)$ and $KO_2(\tilde{X}^2A_2)$

In a comprehensive *ab initio* study of the LiO_2 molecule by Allen and co-workers (90), it has been demonstrated that symmetry breaking of the wavefunction is an important feature to be considered when performing *ab initio* calculations on alkali-metal superoxides and a considerable part of that study (90) was devoted to devising a solution to this problem. Calculations have been performed previously on NaO_2 (91-94) and KO_2 (95), but the only investigation on these molecules to take account of symmetry breaking is that of Horner *et al.* (93) in which the total and relative energies, equilibrium geometries and vibrational frequencies have been computed for the $NaO_2(\tilde{X}^2A_2)$ and $NaO_2(\tilde{A}^2B_2)$ states.

Equilibrium geometries and vibrational frequencies computed in this work at the RHF, UHF and UMP2 levels, for $NaO_2(\tilde{X}^2A_2)$ and $KO_2(\tilde{X}^2A_2)$ are summarised in Tables 8 and 9.

Tables 8 and 9

As may be seen from Table 8, the agreement between the calculated equilibrium geometries for $NaO_2(\tilde{X}^2A_2)$ and the experimentally derived equilibrium geometry is good at the three levels of theory used. It is satisfying to see reasonable agreement between the calculated values obtained in this work and those obtained in a more detailed study (93).

If the vibrational frequencies are considered, the calculated value of $\bar{\omega}_1$ obtained at the RHF level is rather high, when compared to the experimental value, both with the basis sets used in this work and those used in reference (93). Previous calculations on LiO_2 have noted similar poor agreement between calculated RHF $\bar{\omega}_1$ values and the experimental value (44,90). A similar trend was also observed in the calculations performed in this work for KO_2 (see Table 9). The ν_1 vibration in these molecules is effectively an O-O stretch of an O_2^- unit and it appears that inclusion of electron correlation is essential to treat this vibration adequately. In fact, the inadequacy of the Hartree-Fock method to describe O_2^- has been noted elsewhere (96). Other studies also indicate that values of $\bar{\omega}_3$ calculated for $NaO_2(\tilde{X}^2A_2)$ at the RHF level are anomalously small, and values calculated at the UMP2 level are not physically meaningful because of symmetry breaking in the reference function (93). This general trend appears to be present in the results obtained for $NaO_2(\tilde{X}^2A_2)$ and $KO_2(\hat{X}^2A_2)$ shown in Tables 8 and 9. A detailed discussion of this symmetry breaking effect has been presented in references (90) and (93).

Mulliken population analysis of the computed wavefunctions indicates that these superoxide molecules are essentially ionic in their ground states, consistent with previous evidence (34,36,37,62,63,91,95,97). At the RHF(UMP2) level, the charge densities on each centre for $NaO_2(\tilde{X}^2A_2)$ are calculated as $Na^{+0.74}(O_2)^{-0.74}$ [$Na^{+0.68}(O_2)^{-0.68}$], whereas for $KO_2(\tilde{X}^2A_2)$ the corresponding values are $K^{+0.90}(O_2)^{-0.90}$ [$K^{+0.90}(O_2)^{-0.90}$]. The ionic character of these molecules can also be seen by comparing the computed ground state UMP2 equilibrium O-O bond lengths for LiO_2, NaO_2 and KO_2 with that of $O_2^-(X^2\Pi_g)$ [1.30Å(90), 1.38Å and 1.37Å for LiO_2, NaO_2 and KO_2 respectively compared to 1.35Å (98) for $O_2^-(X^2\Pi_g)$]. The calculated UMP2 $\bar{\omega}_1$ values (90), where $\bar{\omega}_1$ is essentially an O-O stretching mode, are also close to the experimental O-O stretch in $O_2^-(X^2\Pi_g)$ (99).

The highest occupied molecular orbitals of NaO_2 are essentially the in-plane (b_2) and out-of-plane (a_2) π^* O_2^- orbitals, the degeneracy of the O_2^- π^* orbitals being removed by the presence of the sodium cation. The valence electronic configuration of $NaO_2(\tilde{X}^2A_2)$ can be written as

$$.................\ (4b_2)^2(1a_2)^1\quad NaO_2\ \tilde{X}^2A_2$$

The $(1a_2)^{-1}$ ionization gives a $^1A_1$ ionic state whereas the $(4b_2)^{-1}$ ionization gives the $^3B_1$ and $^1B_1$ ionic states.

Computed vertical ionization energies to these states from the X^2A_2 neutral state are listed in Table 10 for NaO_2 and Table 14 for KO_2.

Table 10

As may be seen from Table 10, the VIE of band D, (7.28 ± 0.04) eV, observed for the Na + O_3 reaction (Figure 3) and assigned to the first ionization of NaO_2, is in reasonable agreement with the computed VIE for the ionization $NaO_2^+(\tilde{X}^3B_1) \leftarrow NaO_2(\tilde{X}^2A_2)$ of 6.65 eV (CISD + Q value), although the calculated value is lower than the experimental value, as was the case for the alkali monoxide computed VIEs. In fact, a recent ΔSCF HF/6-31G* VIE value reported by Marshall (94) for the same ionization gave 7.16 eV, in good agreement with the experimental value obtained in this work. However, there must be a numerical error in the values quoted by Marshall (94), as in the same paper a ΔSCF HF/6-31G* adiabatic ionization energy value of 7.35 eV is quoted, which is <u>higher</u> than the quoted VIE. Later *ab initio* calculations using a large gaussian basis set including electron correlation via a modified coupled-pair functional method (97), showed that the ground state of NaO_2 has an isosceles triangle structure whereas the ground state of NaO_2^+ has a linear $C_{\infty v}$ structure. Adiabatic and vertical ionization energies were computed as 6.37 and 7.45 eV (97) compared with the experimental values measured in this work of (6.2 ± 0.2) and (7.28 ± 0.04) eV. The binding energy of NaO_2^+ ($^3\Sigma^-$) with respect to $Na^+ + O_2$ was computed as 0.31 eV, with the vertical ionization $NaO_2^+(\tilde{X}^3B_1) \leftarrow NaO_2(\tilde{X}^2A_2)$ lying approximately 0.81 eV above the $Na^+ + O_2$ products (97).

Table 10 also shows that the calculated VIE for the process $NaO_2^+(\tilde{a}^1B_1) \leftarrow NaO_2(\tilde{X}^2A_2)$ places the associated photoelectron band under band A in Figure

3. On comparing spectra recorded from the Na + N_2O and Na + O_3 routes (i.e. Figures 2 and 3), the region of band A was of greater intensity relative to the region of bands B and C in the Na + O_3 spectra than in the Na + N_2O spectra. This would be consistent with the second ionization of NaO_2, i.e. the $\tilde{a}^1B_1 \leftarrow \tilde{X}^2A_2$ ionization, contributing to the 7.70 eV ionization energy region of the spectrum at one third of the intensity of the first NaO_2 band. Also, the $\tilde{b}^1A_1 \leftarrow \tilde{X}^2A_2$ ionization is expected to contribute to this region with a band which maximizes at ≈0.1-0.2 eV higher than the second NaO_2 band (see Table 10). As the NaO_2 ionizations listed in Table 10 are essentially all O2p ionizations from an O_2^- group, their relative intensities are expected to be approximately 3:1:1 ($^3B_1$:$^1B_1$:$^1A_1$) on the basis of the ionic state spin multiplicities.

Grow and Pitzer (44) have calculated the corresponding ionization energies of LiO_2 and have found that the $^1A_1$ ionic state lies between the $^3B_1$ and $^1B_1$ ionic states. A similar result has also been obtained for the valence isoelectronic molecule HO_2 where the $\tilde{a}^1A'$ ionic state has been calculated to lie between the $^3A''$ and $^1A''$ states (100). In comparison, the results obtained at the RHF level for NaO_2^+, shown in Table 10, indicate that the $^1A_1$ state lies slightly above the $^1B_1$ state, although these states could interchange in order at a higher level of calculation. Nevertheless, Table 10 does indicate that the $\tilde{a}^1B_1$ and $\tilde{b}^1A_1$ ionic states are very close in energy.

Although resolved vibrational structure would have been valuable to assist band assignment, the experimental resolution was not sufficient to allow this to be achieved probably because of the contaminating conditions in the ionization chamber arising from the methods used to prepare NaO and NaO_2 and because some of the metal oxide bands were partially overlapped.

Photoelectron Spectra recorded for the K + N_2O and K + O_3 Reactions

The HeI photoelectron spectrum recorded for the K + N_2O reaction in the ionization energy region 4.5-9.0 eV is shown in Figure 4. As in the Na + N_2O case, three closely grouped bands were observed (bands A, B and C). A weaker feature was also observed to higher ionization energy and this was labelled band D. The HeI photoelectron spectrum recorded for the K + O_3 reaction over the same ionization energy range is shown in Figure 5. In contrast to the Na + O_3 case, only two bands (labelled E and F) were resolved associated with reaction products. A summary of the measured VIE's of the observed photoelectron bands, together with the measured onset of the first photoelectron band in each case, is given in Table 11.

Figures 4 and 5

Table 11

Calibration of the spectra shown in Figures 4 and 5 was achieved using the known potassium $(4s)^{-1}$ ionization energy (4.34 eV) (29) and the known position of some atomic features, which have been labelled K^* in these figures. These K^* bands appear at an apparent ionization energy of 6.58 and 6.84 eV on the HeI ionization energy scale (101,102) and, although they proved useful to calibrate the spectral energy scale, they unfortunately masked the structure in the product bands under the conditions used to record the K + O_3 spectra (see Figure 5). These atomic bands are known to arise from $(4s)^{-1}$

ionization of atomic potassium with K 66.2 and 65.3 nm radiation (101,102). The exact mechanism for production of excited potassium that emits this radiation is not well established, although it is thought to be produced when some potassium diffuses into the photon discharge source (101,102).

Ab initio calculated ionization energies of the KO $X^2\Pi$ and $A^2\Sigma^+$ states are shown in Tables 12 and 13 respectively. These tables also list computed r_e and $\bar{\omega}_e$ values for the low-lying accessible ionic states.

The assignment of the K + N_2O spectrum is based on that achieved for the Na + N_2O spectrum and the calculated KO VIEs. The three bands observed in the 7.0-8.0 eV ionization energy region of Figure 4 are assigned as follows.

Band A : $KO^+(X^3\Sigma^-) \leftarrow KO(X^2\Pi)$

Band B : $KO^+(A^3\Pi) \leftarrow KO(X^2\Pi)$

Band C : $KO^+(A^3\Pi) \leftarrow KO(A^2\Sigma^+)$,

where the assignments of bands B and C have been reversed from the Na + N_2O case on the basis of the results of the calculations shown in Tables 12 and 13. The difference between the $KO^+(A^3\Pi) \leftarrow KO(X^2\Pi)$ and $KO^+(A^3\Pi) \leftarrow KO(A^2\Sigma^+)$ VIE values computed at the highest level of theory used (0.13 eV) is not sufficient to allow a firm assignment to be made. However, the preferred assignment is as stated above. It can be seen from Tables 12 and 13 that, after bands A, B and C have been assigned, the next highest ionization is $KO^+(a^1\Delta) \leftarrow KO(X^2\Pi)$ and it is this ionization which is assigned to band D. No further bands that could be associated with KO were observed. As was the case for the Na + N_2O reaction, bands B and C are approximately the same intensity indicating a higher initial population of the A state relative to the X state in the photoionization region.

Assignment of the K + O_3 spectrum (Figure 5) is very much more difficult than assignment of the K + N_2O spectrum because the bands seen from the K + N_2O reaction are not resolved in Figure 5. However, as shown in Table 11, band E occurs to lower ionization energy of the bands A to D seen in Figure 4, and is similar in position to the NaO_2 band seen from the Na + O_3 reaction. It has therefore been assigned to ionization of KO_2 by analogy with assignment of band D in the Na + O_3 reaction to NaO_2. Unfortunately, the room temperature rate constants for the reactions K + O_3 and KO + O_3 do not appear to have been measured, but by analogy with the corresponding sodium reactions, it may be inferred that they will also be high. Hence, a contribution from KO_2 to the K + O_3 experimental spectrum would be consistent with this. It also seems reasonably clear that the band labelled F in Figure 5, spans the region covered by the bands A, B and C in Figure 4. The fact that these features are unresolved suggests that there are other contributions to this energy region, possibly arising from KO_2. Band F is, therefore, assigned to unresolved contributions from bands A, B and C of KO.

Table 14

The calculated vertical ionization energies obtained in this work for KO_2 are summarised in Table 14. As for NaO_2, the measured first vertical ionization energy of KO_2 ((6.01 ± 0.08) eV) is in reasonable agreement with the first vertical ionization energy computed at the highest level of theory used of 6.30 eV (CISD + Q value). Also, the calculated VIEs to the $\tilde{a}^1B_1$ and $\tilde{b}^1A_1$ ionic states indicate that the second and third KO_2 bands will contribute to the 7.0-8.0 eV ionization energy region.

The first adiabatic ionization energy of KO has been measured previously by electron impact mass spectrometry as (7.1 ± 0.2) eV (26) and 7.5 eV (21), and these values are in good agreement with the onset of the first KO band measured in the K + N_2O reaction of (6.9 ± 0.1) eV. It is also interesting to compare the first adiabatic ionization energies (AIEs) of the metal monoxides (MO) and metal dioxides (MO_2) measured in this work. As these oxides are highly ionic and the first ionizations essentially involve removal of an electron from O^- in MO or O_2^- in MO_2, the differences in the first AIEs of MO and MO_2 should be approximately equal to the differences in the electron affinities for O and O_2. This electron affinity difference is 1.02 eV, with the electron affinity of O taken from reference (103) and the electron affinity of O_2 taken from reference (104). The differences in the measured AIEs are (1.2 ± 0.2) eV for KO and KO_2 and (0.9 ± 0.3) eV for NaO and NaO_2 with, as expected, the dioxide occurring at lower ionization energy. Hence, these results are consistent with the qualitative picture of these ionizations involving removal of an electron from an O^- or an O_2^- anion in the metal oxides considered.

A Preliminary Study of the Li + N_2O Reaction

Some photoelectron experiments were also performed on the Li + N_2O reaction. No experiments were carried out on the Li + O_3 reaction because of problems in obtaining a stable lithium evaporation at the same time as a pure beam of ozone over a reasonable length of time. However, ten spectra were recorded from the Li + N_2O route allowing some measurements to be made. The 5.0-9.5 eV ionization energy region of a HeI spectrum recorded for the Li + N_2O reaction is shown in Figure 6.

Figure 6

As can be seen this spectrum consists of two broad bands, which have been labelled A and B. The higher band is masked in Figure 6 by the first band of methyl iodide, which was added as a calibrant (84). However, some spectra were recorded without methyl iodide present, in order to observe this band more clearly. Under these conditions, the spectral energy scale was calibrated using bands associated with the first band of N_2O recorded with HeI_β and HeI_γ radiation (105), as well as the HeI_α $(2s)^{-1}$ ionization of lithium (29). The vertical ionization energies of bands A and B were measured as (8.8 ± 0.2) and (9.4 ± 0.1) eV respectively. The onset of band A was measured as (7.6 ± 0.2) eV, and this was taken as the first adiabatic ionization energy of LiO.

Ab initio calculations on the LiO $X^2\Pi$ and $A^2\Sigma^+$ states and their low-lying ionic states have previously been performed in this laboratory by Cockett (106). SCF and CISD calculations were performed using double zeta basis sets with one d polarization function added to each centre. The results of these calculations are summarised in Tables 15 and 16.

Tables 15 and 16

Because of the broad nature of the two bands seen from the Li + N_2O reaction, it was not possible to use the results in Tables 15 and 16 to give a definitive assignment of the Li + N_2O spectrum. Although bands A and B must correspond to the ionizations $LiO^+(X^3\Sigma^-) \leftarrow LiO(X^2\Pi)$; $LiO^+(A^3\Pi) \leftarrow LiO(A^2\Sigma^+)$ and $LiO^+(A^3\Pi) \leftarrow LiO(X^2\Pi)$, it is not possible to decide exactly how these ionizations can be attributed to the observed bands. A tentative assignment would be that the low energy side of band A arises from the $LiO^+(X^3\Sigma^-) \leftarrow LiO(X^2\Pi)$ ionization, with the rest of the band being attributed to the $LiO^+(X^3\Sigma^-) \leftarrow LiO(A^2\Sigma^+)$ ionization. Band B is then attributed to the $LiO^+(A^3\Pi) \leftarrow LiO(X^2\Pi)$ ionization.

The onset of band A measured in this work, (7.6 ± 0.2) eV, is in good agreement with the ΔSCF CISD AIE for the process $LiO^+(X^3\Sigma^-) \leftarrow LiO(X^2\Pi)$ of 7.57 eV, listed in Table 15. However, previous values from electron impact mass spectrometry were about 1 eV higher at (8.6 ± 0.3) eV (56), (9.0 ± 0.2) eV (57), (8.45 ± 0.20) eV (58), (8.96 ± 0.20) eV (59) and 8.44 eV (21). It is interesting to note that these latter values are generally between the first AIE and VIE measured in this work, close to the steep rise in the photoelectron spectrum, at approximately 8.2 eV shown in Figure 6.

As has been noted earlier, a number of ionization energies of LiO $(X^2\Pi)$ have been calculated by Grow and Pitzer (44), via *ab initio* SCF calculations. Their computed ΔSCF values are in qualitative agreement with those calculated by Cockett (106), listed in Tables 15 and 16, but they are all slightly lower. Comparison of the computed and experimental ionization energies obtained for NaO and KO shows that the LiO ΔSCF ionization energies, which do not include electron correlation contributions, are expected to be lower than calculated ionization energies which include electron correlation and the difference exhibited between the results of Cockett (106) and Grow and Pitzer (44) is therefore consistent with this trend.

Some Comments on the M + O_3 and M + N_2O Reactions, for M = Rb and Cs

The first point to be made concerning caesium and rubidium monoxides, which will be products of these reactions, is that they are both known to have $^2\Sigma^+$ ground states, unlike the lighter alkali metal monoxides which have $^2\Pi$ ground states (40,47-49,51,52). Also, Kolb, Herschbach and coworkers (7,8) have shown that these reactions will give the metal monoxide $X^2\Sigma^+$ state as the dominant product. Obviously, for CsO and RbO the $A^2\Pi$ state cannot be produced by collisional deactivation as it lies above the $X^2\Sigma^+$ state. Also, since the low-lying $^3\Pi$, $^1\Pi$ and $^1\Sigma^+$ states of NaO^+ and KO^+ are calculated to be either weakly-bound or dissociative, then it would seem that it is very unlikely that clearly resolved photoelectron spectral bands will be obtained from these reactions. It may, however, be possible to obtain photoelectron spectra for CsO_2 and RbO_2 from the M + O_3 preparative route, produced from the secondary reaction

$$MO + O_3 \rightarrow MO_2 + O.$$

Some previous work has been performed on rubidium and caesium oxides. Andrews and coworkers have carried out matrix isolation experiments to measure vibrational frequencies of these molecules (35,37,107) and electron impact mass spectrometric experiments have been performed yielding values for the first adiabatic ionization energies of RbO and CsO of 6.69 and 6.22 eV respectively (21,108). As expected, available rate constants for the Rb + N_2O (109) and Cs + N_2O (110) reactions are high, although rate constants do not appear to have been measured for the corresponding M + O_3 reactions.

Application of a Simple Electrostatic Model to Calculate Metal Oxide First Ionization Energies

As the alkali metal oxides are highly ionic, it is possible to use an electrostatic model to calculate their first ionization energies. This method has been used previously to calculate ionization energies of the alkali metal halides (111-113).

If the metal oxide, MO, is purely ionic, then the first ionization energy, which corresponds to removal of an O^- electron, can be expressed in terms of the electronic affinity of O and the coulombic interaction between M^+ and O^- in the following way:-

$$\mathrm{VIE(MO)} = E_a(\mathrm{O}) + \frac{e^2}{4\pi\epsilon_0 r_e} \qquad \ldots\ldots\ldots\ldots\ldots\ldots\ldots\ldots \qquad (5)$$

where r_e is the equilibrium bond length of the neutral MO molecule and $E_a(\mathrm{O})$ is the electron affinity of atomic oxygen. The results of applying equation (5) to LiO, NaO and KO are shown in Table 17.

Table 17

The values listed in this table were derived using the electron affinity of atomic oxygen from reference (103) and the CISD + Q computed equilibrium bond lengths for NaO and KO listed in Tables 1 and 3. For LiO ($X^2\Pi$), a CISD + Q computed value of r_e of 1.679 Å was used (106). As can be seen on comparing the VIEs calculated with this simple model, with the experimental values measured in this work, the agreement is reasonably good. For LiO, NaO and KO, the values computed using equation (5) are too high by 1.2, 0.7 and 0.3 eV respectively. This disagreement probably arises because the metal monoxides are not completely ionic. Also, no account has been taken of charge-dipole interactions, which can be included by adding a polarisation term to equation (5), as has been demonstrated in reference (111) following the method of Rittner (114).

The simple model, outlined above, can also be applied to alkali metal dioxides following the method suggested by Andrews (63). For a MO_2 molecule this involves using equation (5) with the assumption that O_2^- is a sphere with the distance between the cation and anion centres equal to the distance between M^+ and the centre of the O-O bond in a C_{2v} MO_2 structure. The electron affinity of O_2^- is taken from reference (104). The values calculated for LiO_2, NaO_2 and KO_2 with this simple approach are listed in Table 18. As can be seen for the two available vertical ionization energies measured in this work (for NaO_2 and KO_2), the agreement is surprisingly good. Overall, given the simplicity of the method, calculated MO and MO_2 vertical ionization energies obtained with this approach and their changes on going from one alkali metal to another, compare favourably with first ionization energies computed with *ab initio* methods.

Table 18

Dissociation Energies of the Alkali Metal Monoxides and Superoxides

a) Alkali metal monoxides

Suppose the following process is considered

$$\mathrm{Na} + \mathrm{O} \xrightarrow{-D_o} \mathrm{NaO} \xrightarrow{\mathrm{AIE}} \mathrm{NaO}^+ + e^- \xrightarrow{D_o^+} \mathrm{Na}^+ + \mathrm{O} + e^- \quad \ldots\ldots \quad (6)$$

where D_o is the dissociation energy of $\mathrm{NaO}(X^2\Pi)$, D_o^+ is the dissociation energy of $\mathrm{NaO}^+(X^3\Sigma^-)$ and AIE is the first adiabatic ionization energy of NaO.

Taking the first ionization energy of atomic sodium as 5.14 eV (29), then the following relation holds

$$-D_o + \mathrm{AIE} + D_o^+ = 5.14 \text{ eV} \quad \ldots\ldots\ldots\ldots\ldots\ldots\ldots\ldots\ldots \quad (7)$$

If the first adiabatic ionization energy (AIE) of NaO is taken from this work as (7.1 ± 0.1) eV, then equation (7) becomes

$$D_o - D_o^+ = (1.96 \pm 0.10) \text{ eV} \quad \ldots\ldots\ldots\ldots\ldots\ldots\ldots\ldots \quad (8)$$

Clearly, D_o^+ can be determined if D_o is available and *vice versa*.

Although experimental and theoretical values for D_o° (NaO) have been determined as (2.61 ± 0.17) eV (19), (2.76 ± 0.04) eV (20), 2.83 eV (48) and 2.43 eV (50), the most reliable experimental value would appear to be (2.56 ± 0.21) eV (19, 115). This value is based on the data determined in reference (19), an electron impact mass spectrometric study of heated $\mathrm{Na_2O_{(c)}}$, but has been re-evaluated using slightly more reliable thermodynamic and spectroscopic constants (115). This value leads to $D_o^+ = (0.60 \pm 0.31)$ eV, consistent with D_o (NaO^+) of (0.8 ± 0.3) eV determined in a merging beams study of atomic sodium with atmospheric oxygen containing ions (24).

The first ionization energy of atomic potassium is 4.34 eV (29). Hence equation (7) can be rewritten for the potassium monoxide case as

$$-D_o + \mathrm{AIE} + D_o^+ = 4.34 \quad \ldots\ldots\ldots\ldots\ldots\ldots\ldots\ldots\ldots\ldots \quad (9)$$

The first adiabatic ionization energy of KO determined in the present study is (6.9 ± 0.1) eV. Therefore, the difference in the KO and KO^+ dissociation energies can be written as

$$D_o - D_o^+ = (2.56 \pm 0.10)\ \text{eV} \quad \ldots\ldots\ldots\ldots\ldots\ldots\ldots\ldots \quad (10)$$

D_o (KO) has been determined in two mass spectrometric studies as (2.86 ± 0.13) eV (26) and (2.71 ± 0.04) eV (27) respectively. If the most recent value of (2.71 ± 0.04) eV is used in equation (10), then D_o^+ can be derived as (0.15 ± 0.14) eV, consistent with the value of D_o^+, determined from a study of merging beams of atomic potassium with atmospheric oxygen containing ions of (0.3 ± 0.3) eV (24).

A similar calculation for LiO using AIE(LiO) = (7.6 ± 0.2) eV gives

$$D_o - D_o^+ = (2.21 \pm 0.20)\ \text{eV}$$

and using D_o as (3.49 ± 0.06) eV (120), a value of $D_o{}^+$ is obtained as (1.28 ± 0.26) for the ground state of LiO^+.

In summary, it seems that the first adiabatic ionization energies of the metal monoxides measured in this work can be used to yield improved values of the dissociation energies of NaO^+ and KO^+ in their ground electronic states of (0.60 ± 0.31) and (0.15 ± 0.14) eV respectively.

b) Alkali metal dioxides

Similar calculations can be performed for the alkali metal dioxides.

If NaO_2 is considered first, then equation (6) can be rewritten in this case as

$$Na + O_2 \xrightarrow{-D_o} NaO_2 \xrightarrow{AIE} NaO_2^+ \xrightarrow{D_o^+} Na^+ + O_2 \quad \ldots\ldots\ldots\ldots \quad (11)$$

where D_o and D_o^+ are the dissociation energies of NaO_2, ($D_o(Na\text{-}O_2)$), and NaO_2^+, ($D_o(Na^+\text{-}O_2)$), in their ground states.

Using the first AIE of NaO_2 measured in this work of (6.2 ± 0.2) eV, then the differences in the neutral and ionic dissociation energies of NaO_2 is

$$D_o - D_o^+ = (1.06 \pm 0.20)\ \text{eV} \quad \ldots\ldots\ldots\ldots\ldots\ldots\ldots\ldots \quad (12)$$

Unfortunately, no experimental value for $D_o(Na^+\text{-}O_2)$ is available, and the available values for $D_o(Na\text{-}O_2)$ differ widely (see reference (95), Table

8). The lowest experimental value is (1.51 ± 0.22) eV derived by Hynes *et al.* (10) from flame studies, although an upper limit of 1.19 eV was derived in a mass spectrometric study in which no NaO_2 could be detected on evaporation of solid sodium oxides (19,116). In contrast, a value of (2.52 ± 0.09) eV has recently been reported for $D_o(Na\text{-}O_2)$ by Steinberg and Schofield (20) from reanalysis of data from high temperature vaporization experiments on $Na_2O_{(s)}$. However, in the light of these conflicting values, the most reliable value for $D_o(Na\text{-}O_2)$ would appear to be that derived by Partridge *et al.* (121), from a series of *ab initio* calculations which include the effects of electron correlation as 1.61 eV, consistent with the values derived from flame studies by Jensen (11) and Hynes *et al.* (10). If this value is used in equation (12), then D_o^+ can be derived as (0.55 ± 0.20) eV. Alternatively, the computed value of $D_o(Na^+\text{-}O_2)$ of 0.31 eV (97), gives $D_o(Na\text{-}O_2)$ as (1.37 ± 0.2) eV.

In the case of KO_2, the difference between the dissociation energy of the molecule and the ion can be derived as

$$D_o - D_o^+ = (1.4 \pm 0.1)\ \text{eV} \quad \dots\dots\dots\dots \quad (13)$$

using the first ionization energy of atomic potassium of 4.34 eV (29) and the first ionization energy of KO_2 measured in this work as (5.7 ± 0.1) eV.

As in the case of $D_o(Na\text{-}O_2)$, available experimental values of $D_o(K\text{-}O_2)$ vary widely (see Table 8, reference (95)), the lowest value being that of Jensen (11) of (1.8 ± 0.3) eV. The most recent *ab initio* calculations, by Partridge *et al.* (121) give 1.76 eV, which leads via equation (13) to D_o^+ = (0.36 ± 0.10) eV.

If D_o^+ is taken as zero, then $D_o(K\text{-}O_2)$ is (1.4 ± 0.1) eV, consistent with Jensen's value (11), but inconsistent with a value of (2.6 ± 0.2) eV obtained by Steinberg and Schofield (117). Alternatively, use of Jensen's value of $D_o(K\text{-}O_2)$ leads to D_o^+ of (0.4 ± 0.4) eV.

Clearly, in the case of the superoxides, NaO_2 and KO_2, reliable values of $D_o(Na-O_2)$ and $D_o(K-O_2)$ are required to determine $D_o(Na^+-O_2)$ and $D_o(K^+-O_2)$ from equations (12) and (13), although values of (0.55 ± 0.20) and (0.36 ± 0.10) eV are expected to be the most reliable available values based on the MO_2 ionization energies measured in this work and the $D_o(M-O_2)$ values computed in reference (121).

Conclusions

In this work, the low ionization energy region (5.0-10.0 eV) of the HeI photoelectron spectra of the metal oxides NaO and KO have been recorded. Preliminary spectra have also been obtained for LiO. The metal monoxides (M) were prepared for p.e.s. study using the gas-phase $M + N_2O$ and $M + O_3$ reactions.

In the case of NaO and KO, prepared by the $M + N_2O$ method, three bands were observed which could be assigned on the basis of *ab initio* calculations, to ionizations from the $X^2\Pi$ neutral state, to the $X^3\Sigma^-$ and $A^3\Pi$ states, and to ionization from the $A^2\Sigma^+$ low-lying excited state to the $A^3\Pi$ ionic state. For the $Na + O_3$ and $K + O_3$ reactions, an extra band was observed for each reaction which was assigned, on the basis of available kinetic evidence and the results of *ab initio* calculations, to the first ionization energy of the metal superoxide.

The measured first adiabatic ionization energy of each metal monoxide has been used with the available ground state neutral dissociation energy to calculate the dissociation energy in the ground ionic state. For the oxides NaO_2 and KO_2, similar calculations have been hampered by the lack of reliable dissociation energies in the neutral ground states.

One of the main results to be derived from this present work is that in the $Na + O_3$ reaction the $A^2\Sigma^+$ state of NaO is preferentially produced relative to the $X^2\Pi$ NaO state, with an A:X branching ratio of at least 2:1. This result is in accord with the results of recent molecular beam magnetic deflection experiments (7,8). The mesospheric night-glow arises from the $Na^2P \rightarrow Na^2S$ emission, where the ^2P and ^2S states of sodium are produced from the reactions

$$\begin{tikzcd} & \mathrm{Na}(^2P) + O_2 \\ \mathrm{NaO} + O \arrow[ur] \arrow[dr] & \\ & \mathrm{Na}(^2S) + O_2 \end{tikzcd}$$

Laboratory kinetic experiments (118) performed for the $NaO(X^2\Pi) + O$ reaction gave a Na $^2P{:}^2S$ branching ratio which is very small (≤ 0.01) and insufficient to account for the sodium night-glow. However, Herschbach and coworkers have shown, from symmetry correlation considerations (7), that the $NaO(A^2\Sigma^+) + O$ reaction gives a much higher Na $^2P{:}^2S$ branching ratio and this should be able to account for the observed night-glow intensity. Obviously, preferential production of NaO in the $A^2\Sigma^+$ state from the $Na + O_3$ reaction is an essential part of this mechanism and the results of this present work support this conclusion.

Acknowledgements

This work has been supported by the S.E.R.C., the European Community and the Air Force Office of Scientific Research through the European Office of Aerospace Research (EOARD), United States Air Force.

The authors wish to thank Professors D.R. Herschbach, C.E. Kolb, D.L. Hildenbrand, J.L. Gole and C. Yamada for valuable discussions and for sending reprints of unpublished work. Drs. M.C.R. Cockett and B.W.J. Gravenor are also thanked for valuable assistance in the early stages of this work.

References

1. W. Swider, Jr.,

   Planet Space Sci., 17, 1969, 1233

2. (a) E. Murad,

   J. Geophys. Res., 83, 1978, 5525

   (b) E. Murad and W. Swider,

   Geophys. Res. Lett., 6, 1979, 929

   (c) D.R. Bates and P.C. Ojha,

   Nature 286, 1980, 790

3. S. Chapman,

   Astrophys. J., 90, 1939, 309

4. V.W.J.H. Kirchoff, B.R. Clemesha and D.M. Simonich,

   J. Geophys. Res., 84, 1979, 1323

5. S.C. Liu and G.C. Reid,

   Geophys. Res. Lett., 6, 1979, 283

6. C.E. Kolb and J.B. Elgin,

   Nature, 263, 1976, 488

7. (a) D.R. Herschbach, C.E. Kolb, D.R. Worsnop and X. Shi,

   Nature, 356, 1992, 414

   (b) C.E. Kolb, D.R. Worsnop, M.S. Zahniser, G.N. Robinson, X. Shi and D.R. Herschbach

   in: "Chemiluminescence and Chemi-ionization: Gas-Phase Metal Atom Reactions", Ed. A. Fontijn (Elsevier, Amsterdam, 1992, in press)

8. X Shi, D.R. Herschbach, D.R. Worsnop and C.E. Kolb,

   J. Chem. Phys., to be submitted

9. J.L. Gole,

   Opt. Eng., 20, 1981, 5465

10. A.J. Hynes, M. Steinberg and K. Schofield,
J. Chem. Phys., 80, 1984, 2585

11. D.E. Jensen,
J.C.S. Faraday Trans. 1, 78, 1982, 2835

12. R.N. Newman and J.F.B. Payne,
Comb. Flame, 33, 1978, 291

13. R.N. Newman and C.A. Smith,
J. Brit. Nucl. Soc., 12, 1973, 117

14. (a) D.J. Benard, R.C. Benson and R.E. Walker,
Appl. Phys. letts., 23, 1973, 82

(b) R.C. Benson, C.B. Bargeron and R.E. Walker,
Chem. Phys. Letts., 35, 1975, 161

(c) D.J. Benard,
Chem. Phys. Letts., 35, 1975, 167

15. (a) J.W. Ager III and C.E. Kolb,
J. Chem. Phys., 87, 1987, 921

(b) J.A. Silver and C.E. Kolb,
J. Phys. Chem., 90, 1986, 3267

16. J.M.C. Plane,
Int. Rev. Phys. Chem., 10, 1991, 55

17. D. Husain,
J.C.S. Faraday Trans. II, 85, 1989, 85

18. L. Brewer and J. Margrave,
J. Phys. Chem., 59, 1955, 421

19. D.L. Hildenbrand and E. Murad,
J. Chem. Phys., 53, 1970, 3403

20. M. Steinberg and K. Schofield,
J. Chem. Phys., 94, 1991, 3901

21. Values from E.N. Verkhoturov,
Thesis, Moscow State University, 1977
Reported in M.F. Butman, L.S. Kudin and K.S. Krasnov, Zh. Neorg. Khim., 29, 1984, 2150 (English Trans. Russ. J. Inorg. Chem., 29, 1984,1228)

22. P.K. Rol and E.A. Entemann,
J. Chem. Phys., 49, 1968, 1430

23. R.H. Neynaber, B.F. Myers and S.M. Trujillo,
Phys. Rev., 180, 1969, 139

24. P.K. Rol, E.A. Entemann and K.L. Wendall,
J. Chem. Phys., 61, 1974, 2050

25. (a) H. Schmidt, P.S. Weiss, J.M. Mestdagh, M.H. Covinsky and Y.T. Lee,
Chem. Phys. Letts., 118, 1985, 539
(b) J.M. Mestdagh, D. Paillard and J. Berlande,
J. Chem. Phys., 88, 1988, 2398
(c) D. Paillard and J.M. Mestdagh,
J. Chem. Phys., 91, 1989, 6866

26. T.C. Ehlert,
High Temperature Science, 9, 1977, 237

27. M. Farber and R.D. Srivastava,
High Temperatures-High Pressures, 20, 1988, 119

28. K.I. Peterson, P. D. Dao and A.W. Castleman Jr.,
J. Chem. Phys., 79, 1983, 777

29. C.E. Moore, Atomic Energy levels,
Natl. Bur. Stand., Circ. 467 (U.S. Dept. Commerce, Washington, 1949)

30. J. Pfeifer and J.L. Gole,
J. Chem. Phys., 80, 1984, 565

31. J.R. Woodward, J.S. Hayden and J.L. Gole,
Chem. Phys., 134, 1989, 395

32. J.L. Gole,
private communication

33. J.W. Ager III, C.L. Talcott and C.J. Howard,
J. Chem. Phys., 85, 1986, 3263

34. L. Andrews,
J. Phys. Chem., 73, 1969, 3922

35. R.C. Spiker, Jr. and L. Andrews,
J. Chem. Phys., 58, 1973, 713

36. R.R. Smardzewski and L. Andrews,
J. Chem. Phys., 57, 1972, 1327

37. L. Andrews,
J. Chem. Phys., 54, 1971, 4935

38. L. Andrews,
J. Mol. Spec., 61, 1976, 337

39. R.C. Spiker, Jr. and L. Andrews,
J. Chem. Phys., 59, 1973, 1851

40. R.R. Herm and D.R. Herschbach,
J. Chem. Phys., 52, 1970, 5783

41. S.M. Freund, E. Herbst, R.P. Mariella, Jr. and W. Klemperer,
J. Chem. Phys., 56, 1972, 1467

42. R.A. Berg, L. Wharton, W. Klemperer, A. Büchler and J.L. Stauffer,
J. Chem. Phys., 43, 1965, 2416

43. P.A.G. O'Hare and A.C. Wahl,
J. Chem. Phys., 56, 1972, 4516

44. D.T. Grow and R.M. Pitzer,
J.Chem, Phys., 67, 1977, 4019

45. M.J. Clugston and R.G. Gordon,
J. Chem. Phys., 66, 1977, 244

46. J.N. Allison and W.A. Goddard III,
J. Chem. Phys., 77, 1982, 4259

47. J.N. Allison, R.J. Cave and W.A. Goddard III,
J. Phys. Chem., 88, 1984, 1262

48. (a) S.R. Langhoff, C.W. Bauschlicher, Jr. and H. Partridge,
J. Chem. Phys., 84, 1986, 4474
(b) S.R. Langhoff, C.W. Bauschlicher Jr and H. Partridge
in "Comparison of Ab Initio Quantum Chemistry with Experiment for Small Molecules", Ed. R.J. Bartlett (Reidel, Dordrecht, 1985), p. 357

49. S.P. So and W.G. Richards,
Chem. Phys. Lett., 32, 1975, 227

50. E.P.F. Lee, T.G. Wright and J.M. Dyke
Mol. Phys. (in press)

51. D.M. Lindsay, D.R. Herschbach and A.L. Kwiram,
J. Chem. Phys., 60, 1974, 315

52. B.C. Laskowski, S.R. Langhoff and P.E.M. Siegbahn,
Int. J. Quantum Chem., 23, 1983, 483

53. C. Yamada,
personal communication, work in preparation

54. C. Yamada, M. Fujitake and E. Hirota,
J. Chem. Phys., 91, 1989, 137

55. C. Yamada, M. Fujitake and E. Hirota,
J. Chem. Phys., 90, 1989, 3033

56. D. White, K.S. Seshadri, D.F. Dever, D.E. Mann and M.J. Linevsky,
J. Chem. Phys., 39, 1963, 2463

57. J. Berkowitz, W.A. Chupka, G.D. Blue and J.L. Margrave,
J. Phys. Chem., 63, 1959, 644

58. D.L. Hildenbrand,
J. Chem. Phys., 57, 1972, 4556

59. (a) C.H. Wu, H. Kudo and H.R. Ihle,
J. Chem. Phys., 70, 1979, 1815
(b) H. Kudo, C.H. Wu and H.R. Ihle,
J. Nucl. Mat. 78, 1978, 380

60. L. Andrews,
J. Chem. Phys., 50, 1969, 4288

61. R.C. Spiker, Jr. and L. Andrews,
J. Chem. Phys., 58, 1973, 702

62. D.A. Hatzenbuhler and L. Andrews,
J. Chem. Phys., 56, 1972, 3398

63. L. Andrews and R.R. Smardzewski,
J. Chem. Phys., 58, 1973, 2258

64. K.S. Seshadri, D. White and D.E. Mann,
J.Chem. Phys., 45, 1966, 4697

65. H. Hüber and G. Ozin,
J. Mol. Spec., 41, 1972, 595

66. D. Husain, P. Marshall and J.M.C. Plane,
J.C.S. Chem. Comm., 1985, 1216

67. J.A. Silver and C.E. Kolb,
J. Phys. Chem., 90, 1986. 3263

68. D.R. Worsnop, M.S. Zahniser and C.E. Kolb,
J. Phys. Chem., 95, 1991, 3960

69. R.E. Walker and J.E. Creedon,
Combustion and Flame, 21, 1973, 3960

70. D. Husain and P. Marshall,
Combustion and Flame, 60, 1985, 81

71. D. Husain and Y.H. Lee,
Combustion and Flame, 68, 1987, 177

72. J.M. Dyke, A. Morris, G.D. Josland, M.P. Hastings and P.D. Francis,
High Temperature Science, 22, 1986, 95

73. D.K. Bulgin, J.M. Dyke, F. Goodfellow, N. Jonathan, E. Lee and A. Morris,
J. Elect. Spec. Rel. Phen., 12, 1977, 67

74. G.A. Cook, A.D. Kiffer, C.V. Klumpp, A.H. Malik and L.A. Spence,
Adv. Chem. Ser., 21, 1959, 44

75. L.F. Atyaksheva and G.I. Emelyanova,
Zh. Fiz. Khim., 64, 1990, 1741 (Engl. Trans., Russ. J. Phys. Chem., 64, 1990, 934)

76. A.D. McLean and G.S. Chandler.
J. Chem. Phys., 72, 1980, 5639

77. R. Ahlrichs and P.R. Taylor,
J. Chim. Phys., 78, 1981, 315

78. A.J.H. Wachters,
J. Chem. Phys., 52, 1970, 1033

79. B. Roos and P.E.M. Siegbahn,
Theor. Chim. Acta., 17, 1970, 209

80. T.H. Dunning, Jr. and P.J. Hay
in "Methods of Electronic Structure Theory", Ed. H.F. Schaefer III (Plenum Press, New York, 1977) page 1

81. S.R. Langhoff and E.R. Davidson,
Int. J. Quantum Chem, 11, 1974, 61

82. M.F. Guest and J. Kendrick,

GAMESS User Manual, SERC Daresbury Laboratory, CCP1/86/1, 1986

83. J.M. Dyke,

J.C.S., Faraday Trans. II, 83, 1987, 69

84. D.R. Lloyd

J. Physics E 3, 1970, 629

85. W.W. Chase, C.A. Davies, J.R. Downey, Jr., D.J. Frurip, R.A. McDonald and A.N. Syverud,

J. Phys. Chem. Ref. Data, 14, 1985

86. (a) E. Wigner and E.E. Witmer,

Z. Physik, 51, 1928, 859

(b) G. Herzberg,

Molecular Spectra and Molecular Structure. I. Spectra of Diatomic Molecules, van Nostrand, New York, 1950

87. S.R. Langhoff, H. Partridge and C.W. Bauschlicher,

Chemical Physics, 153, 1991, 1

88. F.J. Adrian, E.J. Cochran and V.A. Bowers,

J. Chem. Phys., 59, 1973, 56

89. R.D. Amos and J.E. Rice,

CADPAC: The Cambridge Analytical Derivatives Package Issue 4.1L, Cambridge, 1989

90. W.D. Allen, D.A. Horner, R.L. de Kock, R.B. Remington and H.F. Schaefer III,

Chemical Physics, 133, 1989, 11

91. J.M.C. Plane, B. Rajasekhar and L. Bartolotti,

J. Phys. Chem., 93, 1989, 3141

92. P. Marshall, A.S. Narayan and A. Fontijn,

J. Phys. Chem., 94, 1990, 2998

93. D.A. Horner, W.D. Allen, A.G. Császár and H.F. Schaefer III,
Chem. Phys. Letts., 186, 1991, 346

94. P. Marshall,
J. Chem. Phys., 95, 1991, 7773; 96, 1992, 7872

95. J.M.C. Plane, B. Rajasekhar and L. Bartollotti,
J. Phys. Chem., 94, 1990, 4161

96. M. Krauss, D. Neumann, A.C. Wahl, G. Das and W. Zemke,
Phys. Rev., A7, 1973, 69

97. H. Partridge, C.W. Bauschlicher, M. Sodupe and S.R. Langhoff
J. Chem Phys 96, 1992, 7871

98. D.M. Lindsay, D.R. Herschbach and A.L. Kwiram,
Chem. Phys. Letts., 25, 1974, 175

99. K.P. Huber and G. Herzberg,
Molecular Spectra and Molecular Structure, IV. Constants of Diatomic Molecules (van Nostrand, New York, 1979)

100. J.M. Dyke, N. Jonathan, A. Morris and M.J. Winter,
Mol. Phys., 44, 1981, 1059

101. T.A. Williams and A.W. Potts,
J. Elect. Spec. Rel. Phen., 8, 1976, 331

102. A.W. Potts and E.P.F. Lee,
Chem. Phys. Letts., 67, 1979, 93

103. H. Hotop, R.A. Bennett and W.C. Lineberger,
J. Chem. Phys., 58, 1973, 2373

104. R.J. Celotta, R.A. Bennett, J.L. Hall, M.W. Siegel and J. Levine,
Phys. Rev., A6, 1973, 631

105. D.W. Turner, C. Baker, A.D. Baker and C.R. Brundle,
Molecular Photoelectron Spectroscopy, Wiley, Interscience, London, 1970

106. M.C.R. Cockett,
Ph.D. Thesis, University of Southampton, 1990.

107. L. Andrews, J.T. Hwang, and C. Trindle,
J. Phys. Chem., 77, 1973, 1065.

108. A.B. Gusarov, L.N. Gorokhov and A.G. Efimova,
Teplofiz. Vys. Temp., 5, 1967, 584 (in Russian) (Chem. Abs., 68: 6984z)

109. D. Husain and B.Ji,
Combustion and Flame, 79, 1990, 250

110. D. Husain and B. Ji,
J. Photochem. Photobiol. A53, 1990, 1

111. A.W. Potts, T.A. Williams and W.C. Price,
Proc. Roy. Soc. Lond., A341, 1974, 147

112. A.W. Potts and T.A. Williams,
J.C.S. Faraday II, 72, 1976, 1892

113. A.W. Potts, and E.P.F. Lee,
J.C.S. Faraday II, 75, 1979, 941

114. E.S. Rittner,
J. Chem. Phys., 19, 1951, 1030

115. D.L. Hildenbrand,
private communication.

116. R.H. Lamoreaux and D.L. Hildenbrand,
J. Phys. Chem. Ref. Data, 13, 1984, 151

117. quoted in Table VIII of reference (95)

118. J.M.C. Plane and D. Husain
J.C.S. Faraday II 82, 1986, 2047

119. (a) L. Serrano-Andrés, A. Sánchez de Méras, P. Pou-Amérigo and I. Nebot-Gil
Chemical Physics 162, 1992, 321

(b) L. Serrano-Andrés, A. Sánches de Merás, P. Pou-Amérigo and I. Nebot-Gil
J. Mol. Struct (Theochem) 254, 1992, 229

120. H.M. Rosenstock, K. Draxl, B.W. Steiner and J.T. Herron
J. Phys Chem Ref Data 6(Suppl. 1) 1977

121. H. Partridge, C.W. Bauschlicher, M. Sodupe and S.R. Langhoff
Chem Phys Letts 195, 1992, 200

Figure Captions

Figure 1

Schematic Diagram of Reaction Cell.

Figure 2

HeI Photoelectron Spectrum of the Products of the Na + N_2O Reaction in the 5.0-9.5 eV Region.

Figure 3

HeI Photoelectron Spectrum of the Products of the Na + O_3 Reaction in the 5.0-9.5 eV Region.

Figure 4

HeI Photoelectron Spectrum of the Products of the K + N_2O Reaction in the 4.2-9.0 eV Region.

Figure 5

HeI Photoelectron Spectrum of the Products of the K + O_3 Reaction in the 3.5-9.5 eV Region.

Figure 6

HeI Photoelectron Spectrum of the Products of the Li + N_2O Reaction in the 5.0-9.5 eV Region.

TABLE 1

Calculated Spectroscopic Constants (r_e and $\bar{\omega}_e$) for NaO($X^2\Pi$)[(a)]

Method Used	r_e/Å	$\bar{\omega}_e$/cm^{-1}
RHF	2.053	498.8
CISD	2.068	476.9
CISD + Q	2.077	465.0
Experimental	2.052[b]	492.3[b]
Theoretical (CISD)	2.039[c]	508[c]

[a] See text for computational details

[b] reference (55)

[c] reference (48)

TABLE 2

Calculated Spectroscopic Constants (r_e and $\bar{\omega}_e$) for NaO($A^2\Sigma^+$)[(a)]

Method Used	r_e/Å	$\bar{\omega}_e$/cm^{-1}
RHF	1.955	544.4
CISD	1.961	533.9
CISD + Q	1.965	528.0
Theoretical (CISD)	1.942[b]	533[b]

[a] See text for computational details

[b] reference (48)

TABLE 3

Calculated Spectroscopic Constants (r_e and $\bar{\omega}_e$) for KO($X^2\Pi$)[(a)]

Method Used	r_e/Å	$\bar{\omega}_e$/cm^{-1}
RHF	2.386	390.2
CISD	2.391	382.3
CISD + Q	2.399	375.4
Experimental	-	384[b]
Theoretical (CISD)	2.328[c]	395[c]

[a] See text for computational details; recent calculations on KO($X^2\Pi$) and $A^2\Sigma^+$ shows that the ordering of the two states is critically dependent on inclusion of both dynamic and non-dynamic electron-correlation (48,50,119)

[b] N_2 matrix isolation value (35): where it was assumed that KO($X^2\Pi$) was observed

[c] reference (48)

TABLE 4

Calculated Spectroscopic Constants (r_e and $\bar{\omega}_e$) for KO($A^2\Sigma^+$)[(a)]

Method Used	r_e/Å	$\bar{\omega}_e$/cm^{-1}
RHF	2.281	391.9
CISD	2.275	390.0
CISD + Q	2.280	386.4
Theoretical (CISD)	2.186[b]	429[b]

[a] See text for computational details

[b] reference (48)

TABLE 5

Experimental Band Positions Measured for the Na + N_2O and Na + O_3 reactions

Photoelectron Bands Arising from Reactions between Sodium and N_2O[(a)]		Photoelectron Bands Arising from Reactions involving Sodium and O_3[(a)]	
Band	VIE/eV	Band	VIE/eV
A	7.70±0.06	A	7.70±0.04
B	7.97±0.05	B	7.95±0.07
C	8.20±0.04	C	8.25±0.05
D	Not observed	D	7.28±0.04
Onset of Photoelectron Band = 7.1±0.1 eV (Band A)		Onset of Photoelectron Band = 6.2±0.2 eV (Band D)	

[a] errors quoted are 2σ values

TABLE 6

Calculated Ionization Energies for NaO($X^2\Pi$) and Computed Ionic State Spectroscopic Constants [(a)]

Ionic State	AIE/eV	VIE/eV	$\overline{\omega}_e$/cm^{-1}	r_e/Å
$X^3\Sigma^-$	5.52 (6.78)	5.82 (7.10)	187.3 (207.4)	2.518 (2.528)
$A^3\Pi$	5.86 (7.13)	6.14 (7.40)	58.8 (89.5)	2.778 (2.958)
$a^1\Delta$	7.72 (8.91)	8.02 (9.22)	185.4 (201.7)	2.513 (2.526)
$b^1\Pi$	8.34 (9.53)	8.34 (9.53)	74.7 (114.8)	2.978 (2.938)
$c^1\Sigma^+$	9.87 (10.33)	10.17 (10.63)	183.9 (197.4)	2.509 (2.522)

[a] Values in parentheses are CISD + Q values, the others are RHF values. The spectroscopic constants presented are computed ionic state values. See the text for computational details.
The experimental first AIE and VIE values measured in this work are (7.1 ± 0.1) and (7.70 ± 0.06) eV respectively.

TABLE 7

Calculated Ionization Energies for NaO ($A^2\Sigma^+$) and Computed Ionic State Spectroscopic Constants [(a)]

Ionic State	AIE/eV	VIE/eV	$\bar{\omega}_e/cm^{-1}$	r_e/Å
$A^3\Pi$	5.66 (6.88)	6.13 (7.33)	58.8 (89.5)	2.778 (2.958)
$b^1\Pi$	8.14 (9.28)	8.14 (9.28)	74.7 (114.8)	2.978 (2.938)
$d^1\Sigma^+$	-	9.67 (10.30)	-	unbound

[a] Values in parentheses are CISD + Q values, the others are RHF values. The spectroscopic constants presented are computed ionic state values.
See the text for computational details.

TABLE 8

Calculated and Experimental Equilibrium Geometries and Vibrational Frequencies for $NaO_2(X^2A_2)$ †

Method Used	$r_{Na\text{-}O}$/Å	θ_e/°	$r_{O\text{-}O}$/Å	$\bar{\omega}_1/cm^{-1}$	$\bar{\omega}_2/cm^{-1}$	$\bar{\omega}_3/cm^{-1}$
RHF	2.122	35.6	1.298	1402	448	321^g
UHF*	2.124	35.8	1.305	1369	439	361^g
UMP2**	2.155	37.4	1.380	1010	427	$[982^f]$
Previous Theoretical TZ + d RHF	2.122^a	35.6^a	1.278^a	1456^a	442^a	$292^{(a,g)}$
Previous Theoretical TZ + d, CISD-π	2.139^b	36.5^b	1.340^b	1284^b	434^b	364^b
Experimental	2.1^c	36.9^c	1.33^c	-	-	-
Experimental	2.07^e	-	-	1094^d 1108^e	391^e	333^e

* $\langle S^2 \rangle = 0.78$

** $\langle S^2 \rangle = 0.79$

[a] reference (93)

[b] reference (93)

[c] reference (88)

[d] reference (34)

[e] reference (36)

[f] unphysical vibrational frequency due to symmetry breaking in reference wavefunction (90)

[g] values affected by symmetry breaking

† for details of calculations see text

TABLE 9

Calculated and Experimental Equilibrium Geometries and Vibrational Frequencies for $KO_2(X^2A_2)$ †

Method Used	r_{Na-O}/Å	θ_e/°	r_{O-O}/Å	$\bar{\omega}_1/cm^{-1}$	$\bar{\omega}_2/cm^{-1}$	$\bar{\omega}_3/cm^{-1}$
RHF	2.451	30.7	1.296	1412	337	276^f
UHF*	2.455	30.8	1.302	1379	335	301^f
UMP2**	2.459	32.4	1.372	1007	331	$[873^e]$
Previous Theoretical UHF	2.44^a	30.7^a	1.29^a	-	-	-
Experimental	$(3.3)^b$	$(33)^b$	-	1108^c	307.5^d	ca. 260^d

* $<S^2> = 0.78$

** $<S^2> = 0.79$

[a] reference (95)

[b] estimated values from matrix isolation data - reference (36)

[c] reference (37)

[d] reference (36) : ν_3 absorption not observed, but believed to be obscured by dimer bands in 260 cm^{-1} region (36)

[e] unphysical vibrational frequency due to symmetry breaking in reference wavefunction (90)

[f] values affected by symmetry breaking

† for details of calculations - see text

TABLE 10

Calculated Vertical Ionization Energies (eV) for $NaO_2(X^2A_2)$ †

Method Used	Ionic State		
	X^3B_1	a^1B_1	b^1A_1
RHF	6.85	8.12	8.26
CISD	6.73	7.86	-[b]
CISD + Q	6.65	7.70	-[b]
Previous Theoretical SCF [a]	7.24[a]	-	9.27[a]
Previous Theoretical UMP4* [a]	7.16[a]	-	8.40[a]
Experimental	7.28±0.04(c)	-	-

* UMP4SDTQ/6-31G//HF/6-31G

† for details of calculations - see text

[a] reference (94) : note in this reference the first adiabatic ionization energy seems to have been calculated to be greater than the first vertical ionization energy, that is, the adiabatic I.E. to NaO_2^+ (X^3B_1) is calculated to be 7.35 eV, whereas the vertical I.E. is calculated to be 7.16 eV

[b] problems encountered in convergence of the CI wavefunction

[c] This work; adiabatic value (6.2 ± 0.2) eV

TABLE 11

Measured Photoelectron Band Positions for the $K + N_2O$ and $K + O_3$ Reactions [(a)]

Photoelectron Bands Resulting from Reactions between K and N_2O [(b)]		Photoelectron Bands Resulting from Reactions between K and O_3 [(b)]	
Band	Vertical Ionization Energy/eV	Band	Vertical Ionization Energy/eV
A	7.21±0.08	F	7.33±0.11
B	7.43±0.09		
C	7.71±0.10		
D	8.35±0.11	E	6.01±0.08
Onset of PE band = 6.9±0.1 eV (Band A)		Onset of PE band = 5.7±0.1 eV (Band E)	

[a] See Figures 4 and 5

[b] errors given are 2σ values

TABLE 12

Calculated Ionization Energies for $KO(X^2\Pi)$ and Computed Ionic State Spectroscopic Constants [(a)]

Ionic State	AIE/eV	VIE/eV	$\bar{\omega}_e/cm^{-1}$	r_e/Å
$A^3\Sigma^-$	4.59 (5.81)	4.94 (6.13)	104.7 (110.8)	3.030 (3.000)
$A^3\Pi$	-	5.09 (6.25)	-	unbound
$a^1\Delta$	6.80 (7.92)	7.14 (8.24)	101.2 (105.8)	3.055 (3.012)
$b^1\Pi$	-	7.28 (8.36)	-	unbound
$c^1\Sigma^+$	8.94 (9.44)	9.29 (9.77)	96.3 (98.9)	3.040 (3.032)

[a] Values in parentheses are CISD values, the others are RHF values. The spectroscopic constants quoted are computed ionic state values.
See the text for computational details.
The experimental first AIE and VIE values for KO measured in this work are (6.9 ± 0.1) and (7.21 ± 0.08) eV respectively.

TABLE 13

Calculated Ionization Energies for KO($A^2\Sigma^+$) [(a)]

State	AIE/eV	VIE/eV	$\bar{\omega}_e$/cm^{-1}	r_e/Å
$A^3\Pi$	-	5.24 (6.38)	-	unbound
$b^1\Pi$	-	7.43 (8.49)	-	unbound
$d^1\Sigma^+$	-	8.56 (9.12)	-	unbound

[a] Values in parentheses are CISD values, the others are RHF values. The spectroscopic constants quoted are computed ionic state values. See the text for computational details.

TABLE 14

Calculated Vertical Ionization Energies (eV) for $KO_2(X^2A_2)$ †

Method Used	Ionic State		
	X^3B_1	a^1B_1	b^1A_1
RHF	6.68	7.94	8.15
CISD	6.43	7.55	- [a]
CISD + Q	6.30	7.33	- [a]

[a] problems encountered in convergence of the CI wavefunction

† for details of calculations - see text
The experimental first AIE and VIE values of KO_2 measured in this work are (5.7 ± 0.1) and (6.01 ± 0.08) eV respectively

TABLE 15

Calculated Ionization Energies for LiO($X^2\Pi$) and Computed Ionic State Spectroscopic Constants [(a)]

State	AIE/eV	VIE/eV	$\bar{\omega}_e$/cm^{-1}	r_e/Å
$X^3\Sigma^-$	7.57	7.95	349	2.123
$A^3\Pi$	-	8.45	-	unbound
$a^1\Delta$	10.33	10.68	332	2.13
$b^1\Pi$	-	10.64	-	unbound
$c^1\Sigma^+$	9.77	10.13	339	2.12

[a] reference (106); the values quoted are obtained from CISD calculations The experimental first AIE and VIE values of LiO measured in this work are (7.6 ± 0.2) and (8.8 ± 0.2) eV respectively.

TABLE 16

Calculated Ionization Energies for LiO($A^2\Sigma^+$) [(a)]

State	AIE/eV	VIE/eV	$\bar{\omega}_e$/cm^{-1}	r_e/Å
$X^3\Pi$	-	8.39	-	unbound
$b^1\Pi$	-	10.60	-	unbound
$d^1\Sigma^+$	-	11.54	-	unbound

[a] reference (106); the values quoted are obtained from CISD calculations

TABLE 17

Calculated First Vertical Ionization Energies of the Alkali Metal Monoxides (MO, M=Li, Na, K) using an Electrostatic Model [(a)]

Molecule	VIE/eV	
	Calculated	Experimental
LiO	10.05	8.8±0.2[b]
NaO	8.40	7.70±0.06[b]
KO	7.47	7.21±0.08[b]

[a] See text for further details; calculated values obtained using equation (5)

[b] this work

TABLE 18

Calculated First Vertical Ionization Energies of the Alkali Metal Dioxides (MO_2, M=Li, Na, K) using an Electrostatic Model [(a)]

Molecule	VIE/eV	
	Calculated	Experimental
LiO_2	9.04	-
NaO_2	7.39	7.28±0.04[b]
KO_2	6.46	6.01±0.08[b]

[a] See text for further details; calculated values obtained using equation (5)

[b] this work

Figure 1

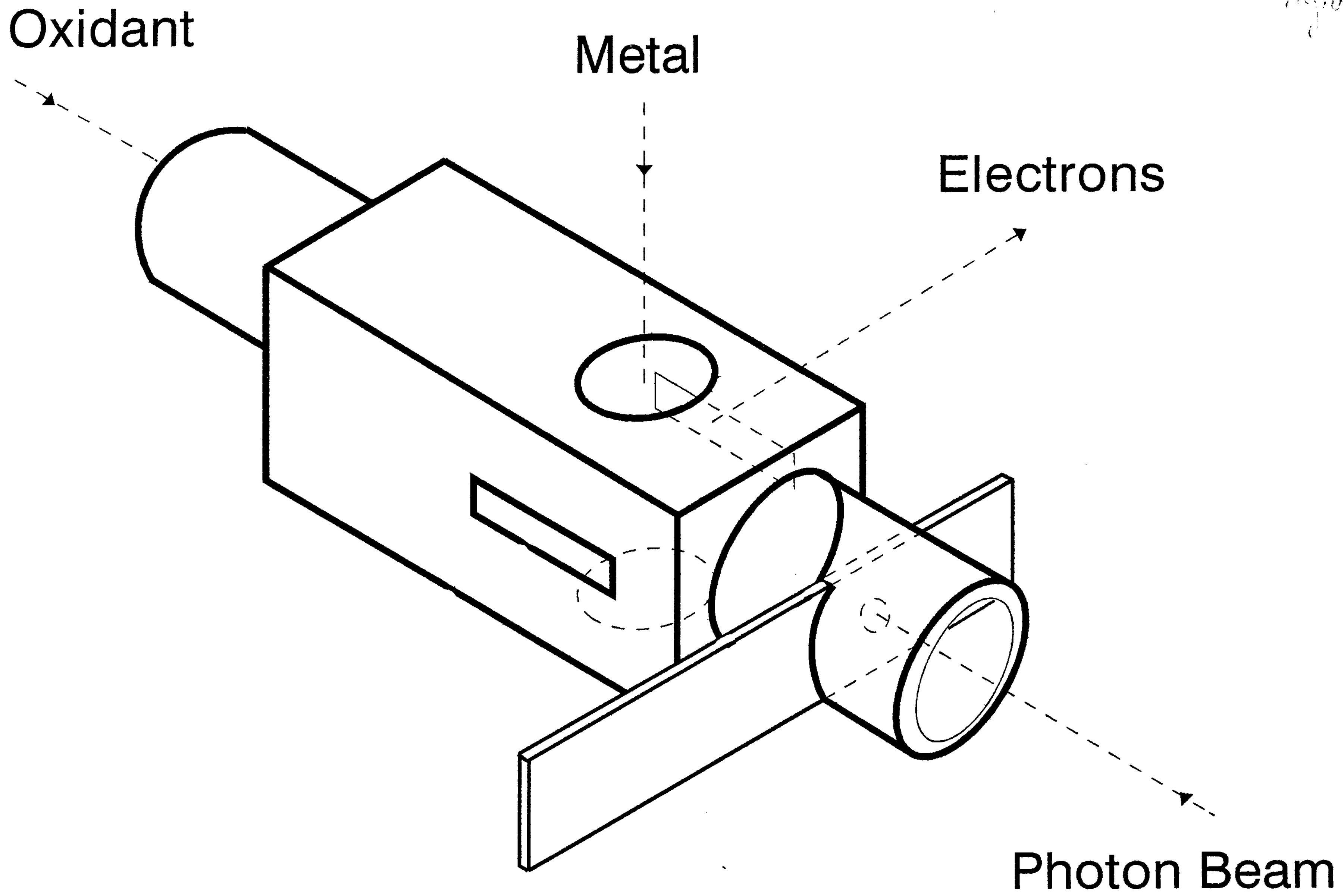

Fig 2

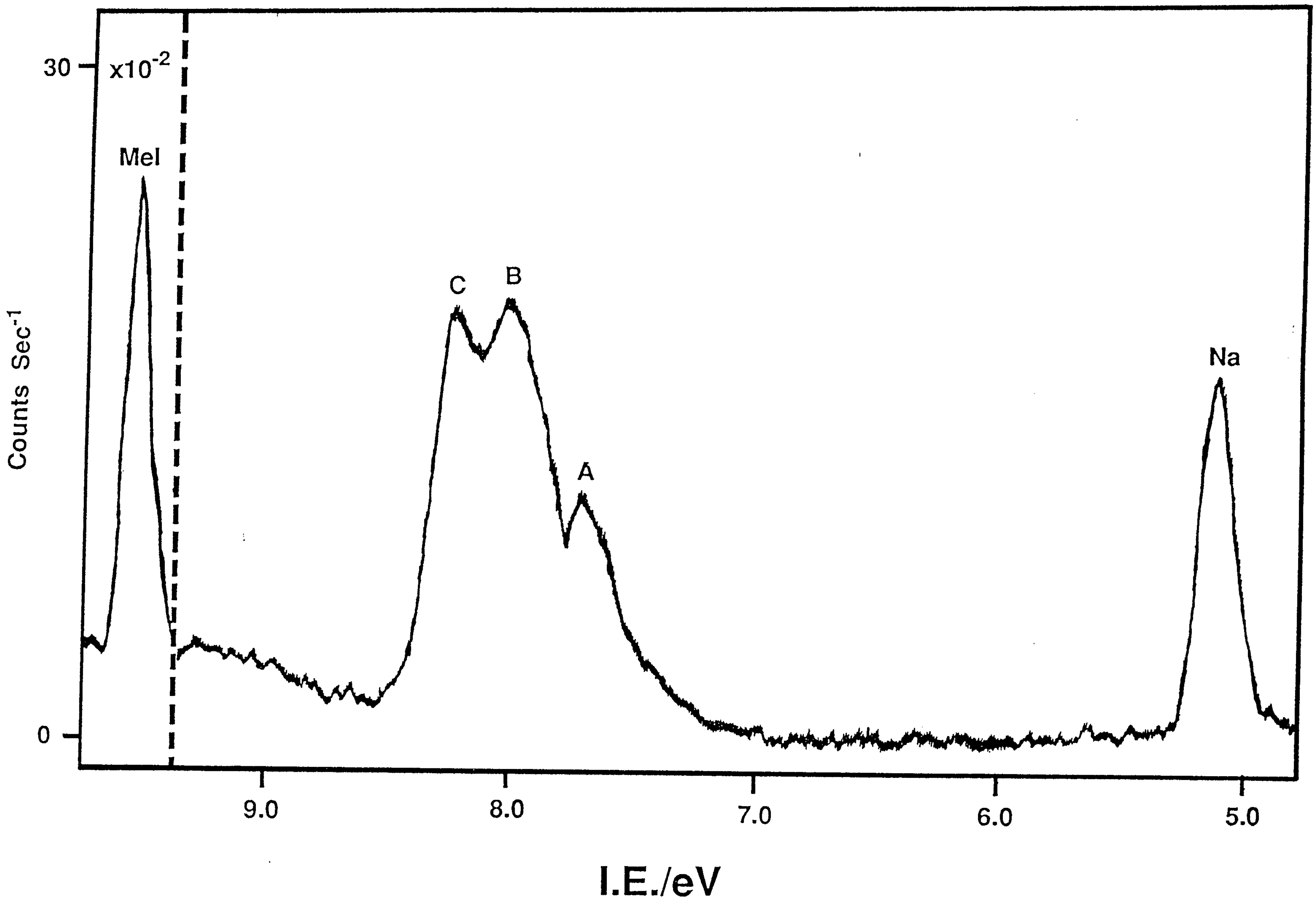

figure 3.

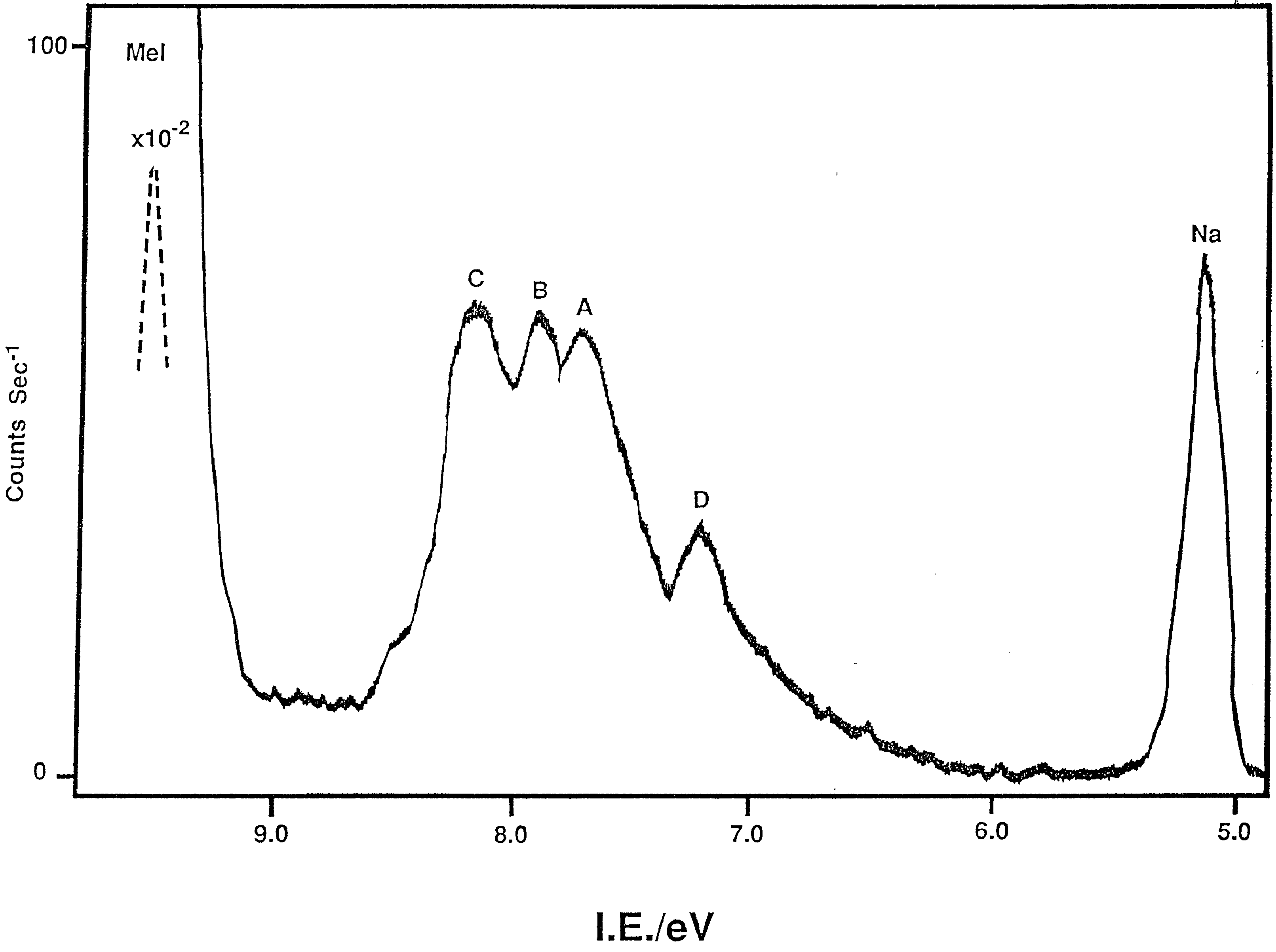

figure 4

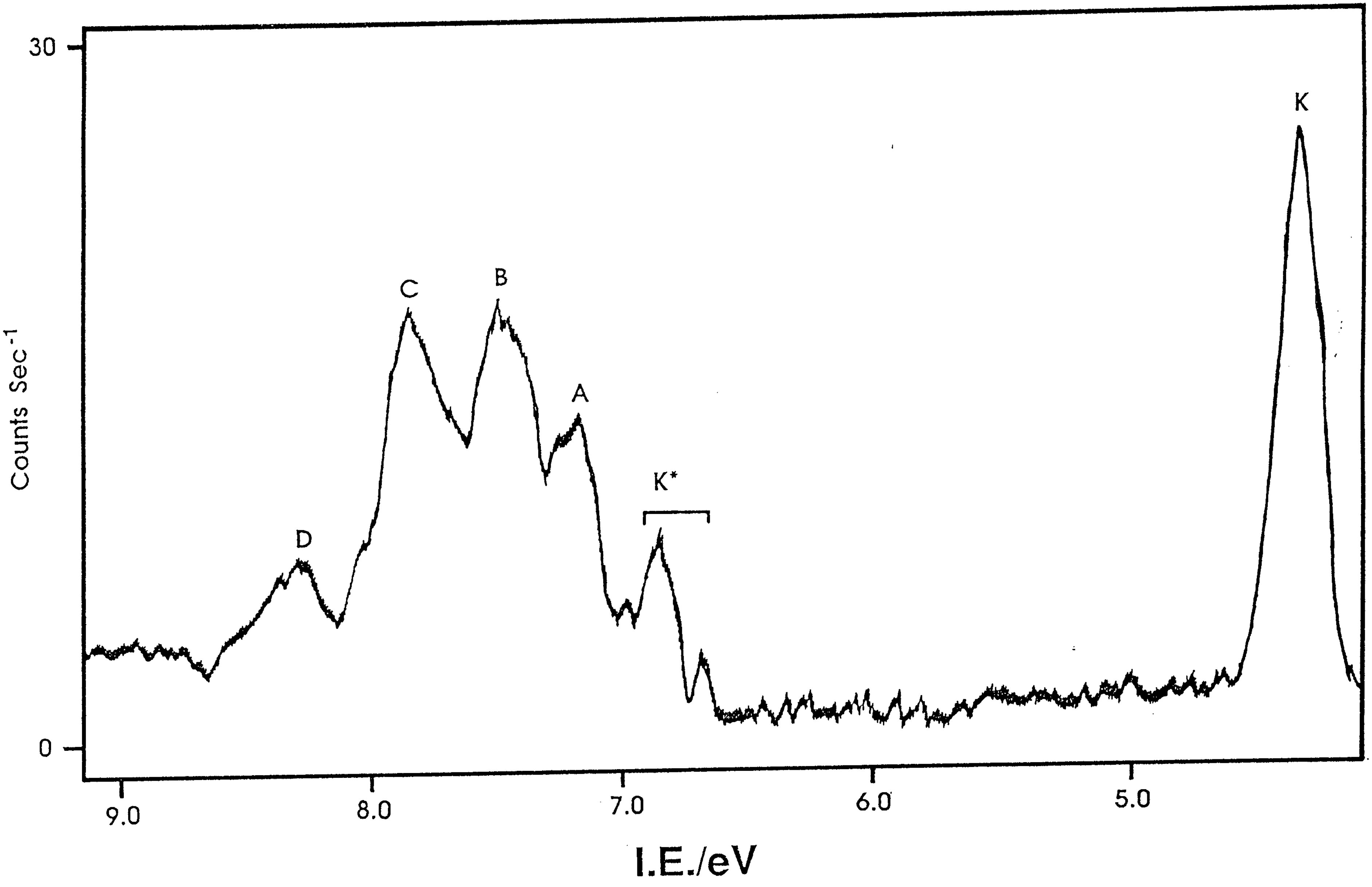

figure 3

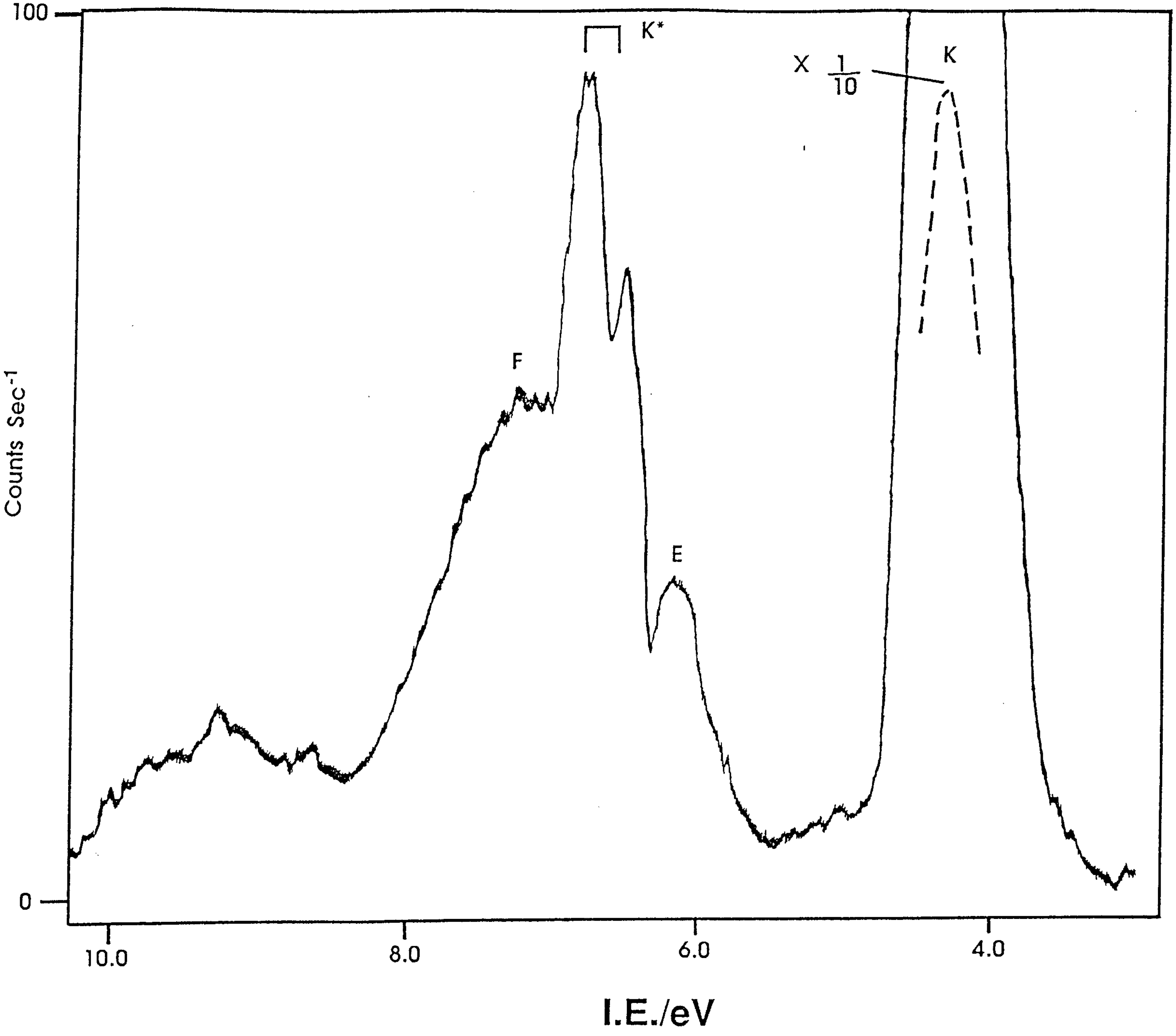

Figure 6

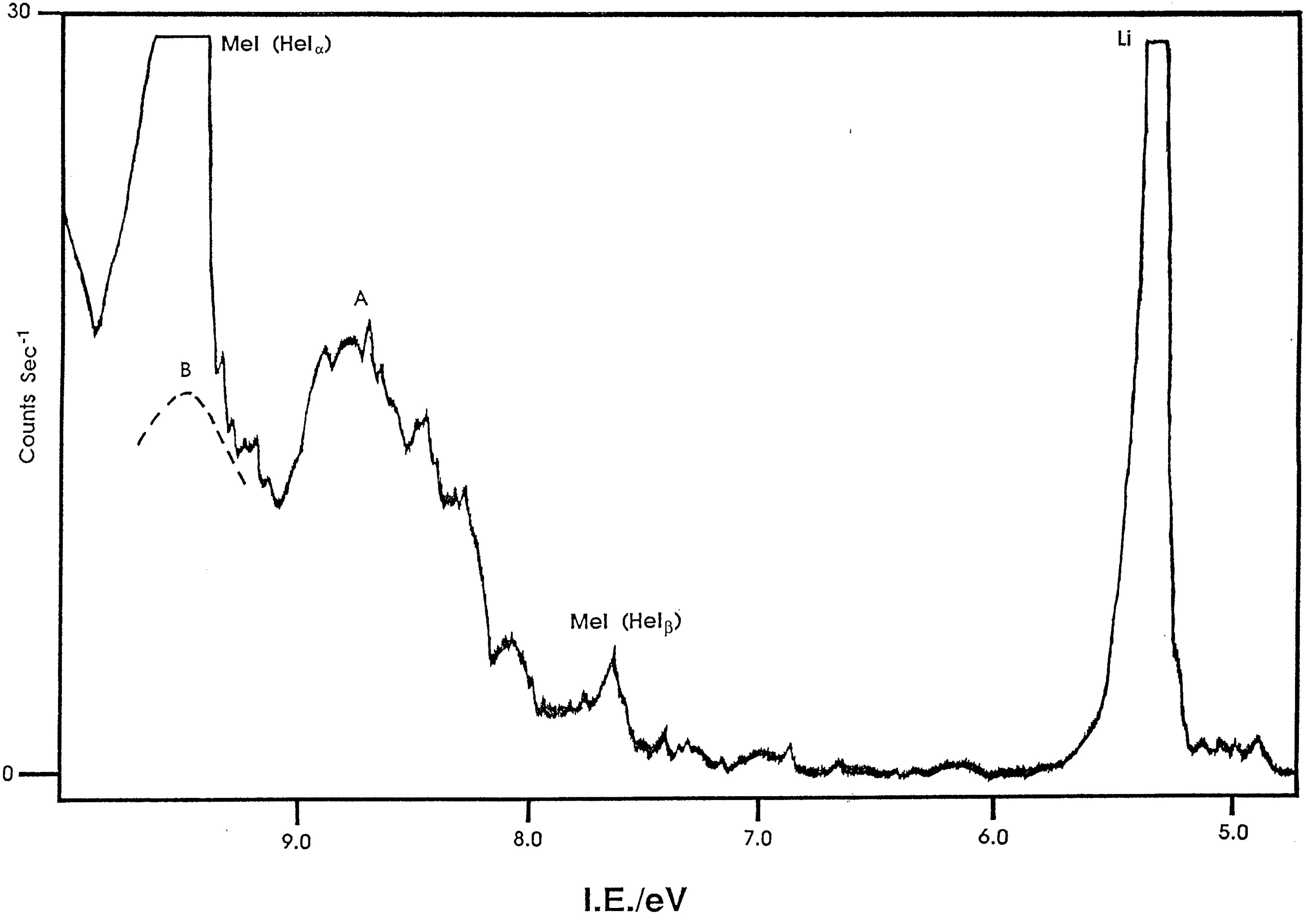
30
0
Counts Sec^{-1}
MeI (HeI$_\alpha$)
A
B
MeI (HeI$_\beta$)
Li
9.0
8.0
7.0
6.0
5.0
I.E./eV